nature reviews neuroscience

https://doi.org/10.1038/s41583-026-01042-4

Review article

Check for updates

Large-scale electrophysiology at single-spike resolution

Joshua H. Siegle [1] & Nicholas A. Steinmetz [2]

Abstract

Recent advances in electrode technology — including the development of Neuropixels and SiNAPS probes — have made it possible to routinely capture spike trains from thousands of neurons distributed across the brain. Widespread dissemination of these tools has not only yielded new discoveries but also changed the way in which neuroscientific questions are asked and answered. In this article, we describe the motivations for collecting electrophysiological recordings on this scale, review the basic physical principles underlying these measurements and discuss key considerations for generating optimally useful datasets. We compare the latest devices for large-scale recordings and address challenges and opportunities in data analysis, rigour, reproducibility and data sharing. Finally, we provide a roadmap for future advances in this space. We argue that widely available hardware, software and protocols are now empowering scientists to perform experiments matched to the scale and complexity of the neural circuits that underlie complex mammalian behaviours.

Sections

[1]Allen Institute/Neural Dynamics, Seattle, WA, USA. [2]Department of Neurobiology & Biophysics, University of Washington, Seattle, WA, USA. e-mail: joshs@alleninstitute.org; nick.steinmetz@gmail.com

Introduction

Neuroscientists face a seemingly daunting task: the number of neurons producing behaviourally relevant signals exceeds our capacity to record from them by many orders of magnitude. The human brain contains roughly 86 billion neurons, whereas a mouse brain has around 70 million[1]. This makes the task of inferring brain function from recordings of hundreds or even thousands of neurons akin to discerning a movie's storyline by watching a handful of pixels on a screen. Yet similar to the flickering of a pixel inside a digital display, the state of an individual neuron is highly correlated with that of its neighbours, as well as with the broader 'plot' – the sequence of internal states and behaviours that guide an animal towards its goals. Thus, recording from the right combination of neurons, coupled with models that capture how their activity relates to that of their unobserved neighbours, should make it possible to infer the presence of global activity patterns despite a limited sample size. This may allow us to gain a comprehensive understanding of the neural basis of behaviour without needing to record every spike from every neuron, a feat that may never be achievable[2]. For example, the position of a rat in a 2D environment can be reconstructed to within 1 cm from the spike trains of around 100 pyramidal cells in the CA1 region of the hippocampus[3], which represent fewer than 0.1% of the neurons in this structure[4]. Studies have shown that behaviourally relevant variables can be extracted from similarly small populations in other circuits[5–8], suggesting that this redundancy is a general feature of neural activity.

If such insights can be gained from recordings of just a few dozen neurons, what new principles might emerge when we can monitor much larger populations? Recent advances in extracellular electrophysiology, driven largely by the application of complementary metal-oxide semiconductor (CMOS) manufacturing processes to electrode fabrication, are beginning to provide answers to this question[9]. Devices containing hundreds of recording sites spread over several millimetres of tissue can uncover population-level structures in neuronal activity that would remain hidden with more limited sampling. A striking example is the toroidal manifold formed by the activity of specialized 'grid' cells in the rat medial entorhinal cortex, the discovery of which required simultaneous recordings from more than a hundred cells within small regions called 'grid modules'[10].

Perhaps even more impactful than the denser sampling within individual brain regions that these technologies enable is their ability to record from hundreds or thousands of neurons across multiple brain regions simultaneously. By generating far richer and more spatially distributed data in each experiment, researchers can now assemble substantially larger datasets within a single study. This has given rise to a new experimental paradigm: the electrophysiological survey. Such surveys systematically sample spiking activity under similar behavioural conditions in different populations of neurons. Surveys may aim for broad coverage across the brain[11–14] or focus on denser sampling within specific regions[15–18]. With the latest tools in hand, a single experimenter can now record the activity of tens of thousands of neurons, whereas coordinated teams can generate datasets containing hundreds of thousands[19]. These surveys have raised fundamental conceptual questions for the field: to what extent cognitive and motor functions of the brain rely on distributed networks versus localized processing[20,21]; and whether the very concept of a brain 'region' has outlived its usefulness[22].

The brain activity patterns that underlie perception and cognition are not only widespread, they are fast. The timescales of neuronal spiking are typically dozens to hundreds of milliseconds[23–25], and relevant frequency ranges span from very slow[26] to more than 100 Hz (ref. 27). A notable example of such fast activity patterns are sharp-wave ripples in the hippocampus, which last only around 100 ms but within which the precise ordering of spiking events across neurons may contain information about past experiences or future plans[28]. A recent preprint has suggested that precise temporal ordering of neuronal spiking on the timescale of dozens of milliseconds may be a general feature across the brain[29]. Such fast timescales of neural activity are to be expected, given that full sensorimotor behaviours, from stimulus onset to action initiation, can unfold over just dozens or hundreds of milliseconds[30,31].

Electrophysiology is currently the technique that best matches the brain's intrinsic spatial and temporal scales, capturing both the distributed structure and fast dynamics of neuronal activity (Fig. 1). Thanks to the widespread availability of easy-to-use recording devices, neuroscience has entered a new era of democratized large-scale electrophysiology. This is further supported by refined surgical methods for accessing the brain, open-source software for data acquisition and analysis, and a growing ecosystem of publicly available datasets. As a result, the ability to perform science at this scale, whether by data collection or analysis, has become accessible to a far broader segment of the community than ever before.

In this Review, we first outline the physical properties of the signals associated with spikes, and explain why implanted electrodes are the best available tool for measuring them. We then survey the devices that enable recordings from more than a thousand channels

Fig. 1 | Comparing the spatial and temporal scale of neural recording techniques. A fundamental goal of systems neuroscience is to uncover the patterns of neural activity that generate behaviour at the scale of the whole organism. **a**, Although a mouse brain contains approximately 30 million neurons (excluding cerebellar granule cells)[1], many aspects of behaviour can be described using far fewer variables. An instructive analogy, depicted here, is decoding the content of a movie: it is not necessary to observe every pixel to understand what is happening, although interpretation becomes easier when more pixels are available over larger spatial scales, allowing the observer to track the action in real time. To illustrate this idea, we can visualize the fraction of pixels in a 1,280 × 720 movie that would be simultaneously accessible via four different recording modalities. For each modality, we depict an approximate field of view (FOV; the sampled spatial extent) overlaid on a mouse brain slice (left panel), one frame of the movie as 'seen' by each modality, assuming ~30 million neurons are compressed into ~900,000 pixels (middle panel), and how the dynamic movie would appear, given each modality's spatial and temporal sampling constraints (right panel). **b**, An analogue for extracellular electrophysiology, which can currently record from around 3,000 neurons[67], would detect rapid changes in around 90 pixels distributed in 3 locations. Although the static view is relatively uninformative, the presence of a brown character moving from left to right is readily discernible in the pixels × time array. **c**, An analogue for voltage imaging, which can currently record from around 300 neurons at a time[77], also detects fast changes in the scene but over a much smaller spatial scale, making interpretation more difficult. **d**, The calcium imaging analogue can sample around 30,000 pixels at once (equivalent to the 1 million neurons captured by this technique[69]), but much of the structure is obscured by motion blur due to the relatively low sampling rate. **e**, Functional ultrasound can capture a field of view that spans nearly half the mouse brain[305], but records haemodynamic signals (analogous to display temperature) rather than the activity of individual neurons. In the case of calcium imaging and functional ultrasound, rapid fluctuations in activity are difficult to capture on single trials, and emerge only after extensive averaging. fps, frames per second.

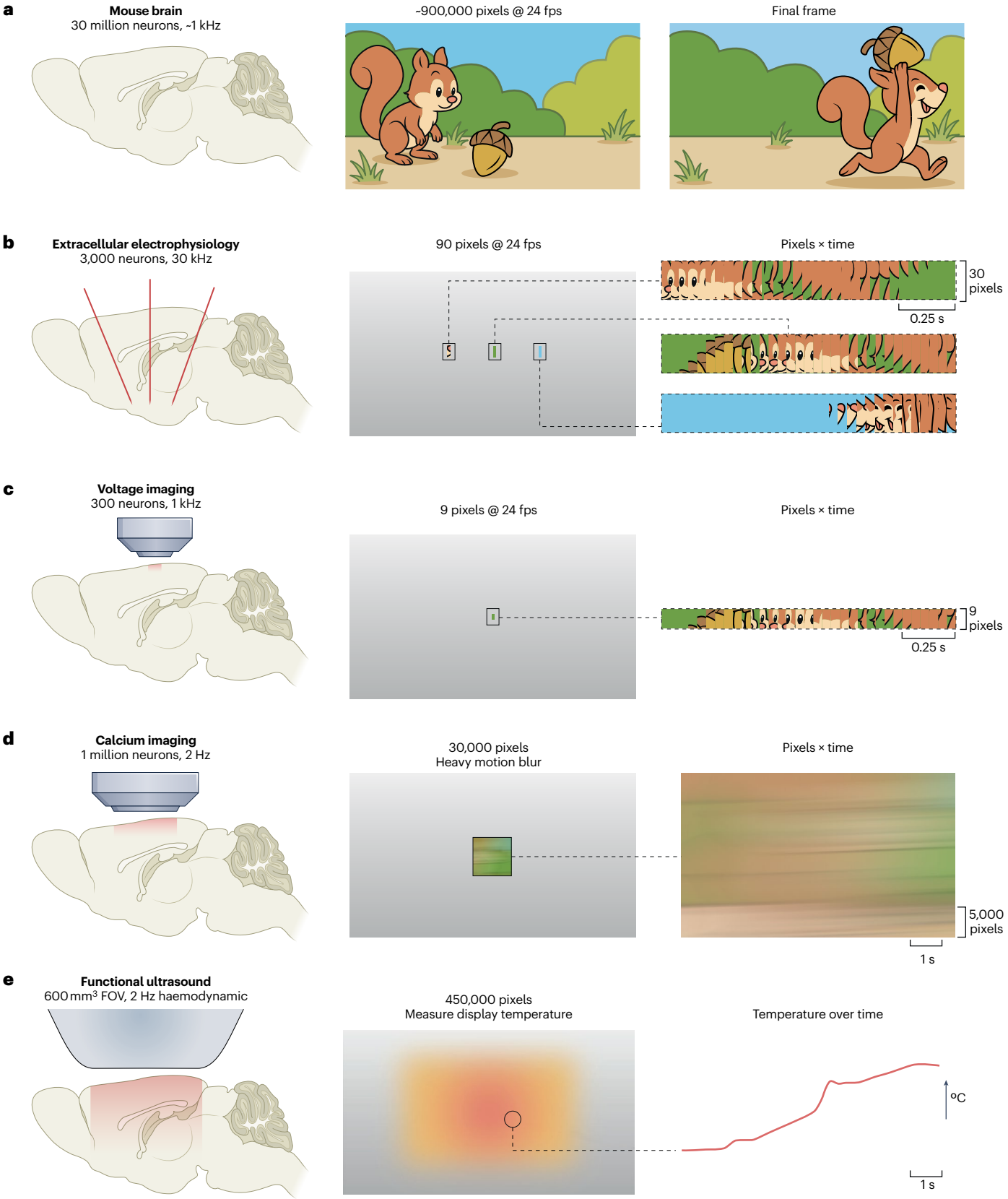
a
Mouse brain
30 million neurons, ~1 kHz
~900,000 pixels @ 24 fps
Final frame
b
Extracellular electrophysiology
3,000 neurons, 30 kHz
90 pixels @ 24 fps
Pixels × time
30 pixels
0.25 s
c
Voltage imaging
300 neurons, 1 kHz
9 pixels @ 24 fps
Pixels × time
9 pixels
0.25 s
d
Calcium imaging
1 million neurons, 2 Hz
30,000 pixels
Heavy motion blur
Pixels × time
5,000 pixels
1 s
e
Functional ultrasound
600 mm³ FOV, 2 Hz haemodynamic
450,000 pixels
Measure display temperature
Temperature over time
°C
1 s

simultaneously, along with associated tools and key methodological innovations. Next, we discuss the issues that arise when working with data at this scale and highlight how a blossoming ecosystem of freely available software and datasets is addressing many of these challenges. Finally, we look ahead to avenues for scaling these technologies and making electrophysiology even more powerful.

Recording electrical brain signals

Action potentials, or 'spikes', arise from the rapid flux of Na^+ and K^+ ions across neuronal membranes, are initiated at the soma or axon initial segment and propagate reliably along the entire axon. Spikes serve as the fundamental signals coordinating brain-wide activity on millisecond timescales. For understanding the neural basis of behaviour, they are therefore indispensable. There are multiple complementary ways to approach the problem of detecting spikes in the brain, each with their own advantages.

Detecting spikes with implanted electrodes

Penetrating electrodes of the appropriate size and impedance can reliably capture fluctuations in the electric potential fields that propagate in the space between neurons[32,33]. The transmembrane ionic flux associated with each spike drives current through the resistive extracellular space, which can be measured as a change in voltage relative to a reference electrode. These voltage differences (extracellular potentials) can be picked up by a simple conductor (such as a metal wire) and an amplifier, a set-up that has been used to record spikes from individual neurons for nearly a century[34,35]. Yet the physical properties of these signals pose significant challenges when attempting to scale up recordings.

Extracellular potentials decay rapidly, making electrode proximity to the spiking neuron a fundamental requirement for high-fidelity spike recording[36,37]. For a simplified dipole source (which approximates a neuron), the electric voltage (V) falls off with the inverse square of the distance (r) from the source in most directions[33]. Consequently, beyond around 50 µm from the electrode, recorded spike amplitudes typically fall below the levels required for accurate spike sorting[38,39]. The necessity for close proximity between the electrode and the neuron raises concerns about tissue damage. Minimizing the probe size and optimizing insertion procedures can mitigate acute damage[40], but the surviving tissue can still respond adversely on both short and long timescales. For example, cortical spreading depression can occur immediately after insertion[41], whereas glial scarring may develop over hours to days[42,43]. Thus, the need to keep the diameter of probes as narrow as possible (<100 µm), and the shanks of devices sufficiently far apart (>250 µm) when multiple shanks are present, places limits on the electrode packing density that can be achieved.

The geometry and biophysics of the recorded neuron strongly influence its extracellular signature. Asymmetric neurons, such as cortical pyramidal cells, generate pronounced dipoles because current sources and sinks are spatially separated along the somatodendritic axis. This produces potentials that are generally detectable tens of micrometres away[32,44] (Fig. 2). Recordings near membrane regions distant from the site of current influx, such as apical dendrites or axons, often capture 'return currents', which appear as positive voltage deflections[33,44]. With sufficient proximity, electrodes can therefore detect spiking-related activity not only from cell bodies but also from axons[45–53], dendrites[54,55] and synaptic termination fields[56,57]. In some cases, waveform features related to these morphological elements can help to identify cell types[54]. However, morphologically similar classes, such as D1 and D2 striatal neurons, remain indistinguishable via their spike waveform[58].

The properties of the electrode also shape the recorded signal. A key parameter is the size of the recording site: larger sites average the potential over a wider area, which can reduce the measured amplitude of a highly localized potential[59–61]. Conversely, smaller sites can more accurately sample the peak of the potential but have higher impedance, which increases their thermal noise[55,62]. This creates a trade-off between spatial resolution and signal-to-noise ratio. The other primary characteristic of the electrode is its material, which affects impedance and therefore noise, but also bears on its biocompatibility, stability and optical sensitivity. Noise levels are determined by a combination of thermal noise at the electrode–tissue interface, artefact-inducing external sources and processing hardware. Thermal noise is roughly proportional to the inverse square root of the surface area of the electrode and can therefore be reduced through coatings that increase the effective surface area[63,64] or by otherwise designing the electrode to have a large effective area[65]. External noise sources, as from radio-frequency interference or light-induced electrical signals, can be mitigated with amplifiers that are positioned close to the electrode or with certain probe design choices[66]. Effective noise introduced by digitization can be minimized with high bit-depth analogue-to-digital converters.

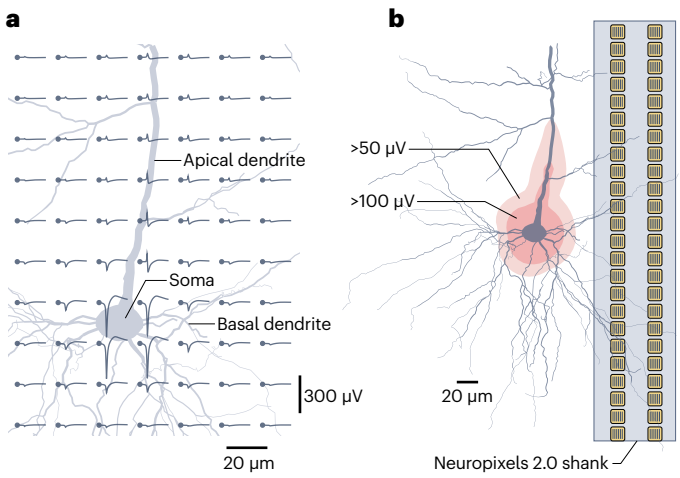

Fig. 2 | Principles of extracellular potential recordings. Simulated extracellular potentials can be used to estimate the detectable range and spatial profile of a spike. **a**, A model of an adult rat cortical layer 5b pyramidal cell[306] was used to simulate spike waveforms at different locations relative to the soma. Note the rapid decay in spike amplitude with increasing distance from the soma and the polarity reversal along the apical dendrite. **b**, The same neuron model as in panel **a**, highlighting the region over which the extracellular potential exceeds 100 µV (an amplitude that would be readily isolated by an extracellular electrode array) or 50 µV (an amplitude near the detection threshold). A Neuropixels 2.0 shank is included for scale. Adapted with permission from ref. 33, Cambridge Univ. Press.

Detecting spikes via imaging

Imaging approaches to detecting the spiking of individual neurons have advanced rapidly in recent years and hold great promise for recording from large populations at single-spike resolution. Calcium imaging has been used to record from tens of thousands of neurons simultaneously across broad areas of the cortex with single-neuron resolution[67,68] and even from up to around 1 million neurons with multi-beam light

bead imaging[69]. However, the reliance of these techniques on calcium indicators imposes fundamental limitations. Calcium indicators have a decay time of greater than 100 ms (ref. 70), making recovery of individual spikes challenging[71]. As a result, methods for translating calcium dynamics into spiking tend to focus on recovering average firing rates, rather than precise spike timing[72–76].

For single-spike imaging, the use of voltage indicators and high frame rates provides an appropriate temporal resolution and signal-to-noise ratio. However, the field of view is typically limited to achieve sufficiently high frame rates[77]. In addition, light scattering limits imaging depths to approximately 500 µm for two-photon approaches and approximately 1 mm for three-photon approaches[78], unless bulky lenses are implanted into the tissue[79]. Thus, voltage imaging has so far been restricted to dozens to hundreds of neurons at a time[77,80], and the path to scaling further is unclear. Moreover, scaling to multiple brain regions is generally a challenge, as multi-field of view two-photon microscopes[81–83] add tremendously to the complexity and expense of the apparatus. By contrast, electrophysiology can straightforwardly be expanded to multiple probes targeting a range of brain regions[67].

Imaging approaches that rely on genetic engineering to induce the expression of exogenous fluorescent proteins have the substantial advantage of being targetable to selected cell types. By contrast, identifying the type of neuron with the features available to electrode recordings, such as waveform shape and firing rate, is possible only in certain situations or with limited precision[84–92]. Thus, additional techniques performed alongside electrical recording are typically needed to identify cell types, such as antidromic stimulation to identify neurons by projection target or optotagging to identify neurons by genetic type. However, the requirement to perform genetic modification limits imaging to a subset of species, and genetic engineering is itself an invasive approach that risks damaging the system under study[93].

Given that imaging and electrophysiology have complementary strengths and limitations, integrating them within the same experiment can be especially powerful for addressing certain experimental goals[94,95]. For example, pairing large-scale electrophysiology with 'widefield' (cortex-wide) calcium imaging of mesoscopic cortical dynamics in mice can reveal the link between neurons' spikes and the global dynamics in which they participate[96,97]. This multimodal strategy has uncovered the learning-dependent mapping of cortical dynamics to striatal spiking[98], the state dependence of cortico-cerebellar connectivity[99], the simultaneous propagation of travelling waves through cortex, striatum, thalamus, and midbrain[100], and, in a recent preprint, the basis of visual cortical spiking variability in cortex-wide shared fluctuations[101].

Other considerations

In studying the neural basis of behaviour, it is desirable for experimental subjects to engage in behaviours with as few restrictions as possible, which typically results in motion of the brain within the skull, even for experiments with a head-fixed set-up[102,103]. Despite a long history of creative strategies to stabilize brain tissue[104], this remains a challenging problem in most preparations: even the heartbeat may move brain tissue enough to considerably alter a neuron's waveform[105]. For electrode recordings, such motion may lead to errors in determining which spikes arise from which neurons. However, both the material properties of the probe and post hoc computational algorithms can be adapted to address this challenge.

Finally, for a recording technology to be scientifically impactful, it must be simple and robust to employ as well as accessible. Ideally, the device should be 'plug and play' without complex set-up or assembly requirements, and should be insertable into the brain without great skill or extensive practice. The device must be manufacturable at scale and at costs affordable to neuroscience laboratories. Finally, it should come with extensive open software and protocols that make it easy to experimentally adopt and to analyse the data. Taking all of these factors into account, electrode array recordings remain the tool of choice to achieve single-spike resolution in populations of neurons from arbitrary brain locations with minimal tissue damage.

Methods for large-scale electrophysiology

We here define 'large-scale electrophysiology' as simultaneous sampling from at least 1,000 implanted electrodes. This level of parallel readout is essential for capturing the rich, distributed neural dynamics that make electrophysiology so powerful. Although there are only a handful of devices that have surpassed this threshold to date, we expect that recordings from more than 10,000 electrodes will be routine by the end of the decade.

Devices

Large-scale electrophysiology devices hail from two lineages[106]. The 'Utah array' evolved from simple microwire bundles, and each array consists of 64–100 micromachined shanks terminating in an exposed metal tip[107,108] (Fig. 3a). Utah arrays are widely used and have set the standard for brain–computer interfaces. Scaling in this lineage can be achieved by increasing the number of shanks per device or by implanting multiple devices in parallel. A recent adaptation directly couples the microwires to a 2D amplifier circuit, enabling recordings from 1,300 electrodes in rat neocortex[109]. In primates, a set of sixteen 64-channel Utah arrays have been implanted along the ventral visual stream, achieving simultaneous readout from 1,024 electrodes[110,111]. Further scaling of these devices is best suited for such larger animals, owing to the size of the connector and cabling system.

The second lineage traces its origins back to the 'Michigan array', which was fabricated by depositing conductive metal traces on a silicon substrate[112]. Unlike Utah arrays, each shank of a Michigan array may contain many electrical contacts. The channel count is tightly constrained by the shank width, as the metallic traces that convey signals away from each electrode cannot overlap. As larger shank widths cause increasing levels of tissue damage[113–115], scaling beyond 1,000 channels has required a dramatic decrease in the trace size[116] or the stacking of four 256-channel modules (with 64 channels per shank)[117,118]. Such 'passive' silicon electrode arrays are also limited by the challenge of connecting the electrodes to external readout circuits: for 1,000 or more channels, this requires large printed circuit boards that are impractical in many experimental settings. However, this connectorization challenge has been addressed by leveraging CMOS manufacturing, which allows electrodes, amplifiers and analogue-to-digital converters to be integrated into a monolithic chip. CMOS technology is essential for the mass production of computer processors, camera sensors and other integrated circuits. Despite its ubiquity, its application to custom neuroscience devices has been limited by high manufacturing costs and the relatively small market size. Nevertheless, CMOS technology offers substantial advantages for large-scale electrophysiology applications. For example, it enables multiplexed signal readout, which greatly increases the number of electrodes that can be placed on a narrow shank.

Currently, the most widely used CMOS electrode arrays are Neuropixels 1.0 (Fig. 3b). These probes pack 960 electrodes onto a shank 70 µm wide[119], 384 of which can be read out in parallel. This compact

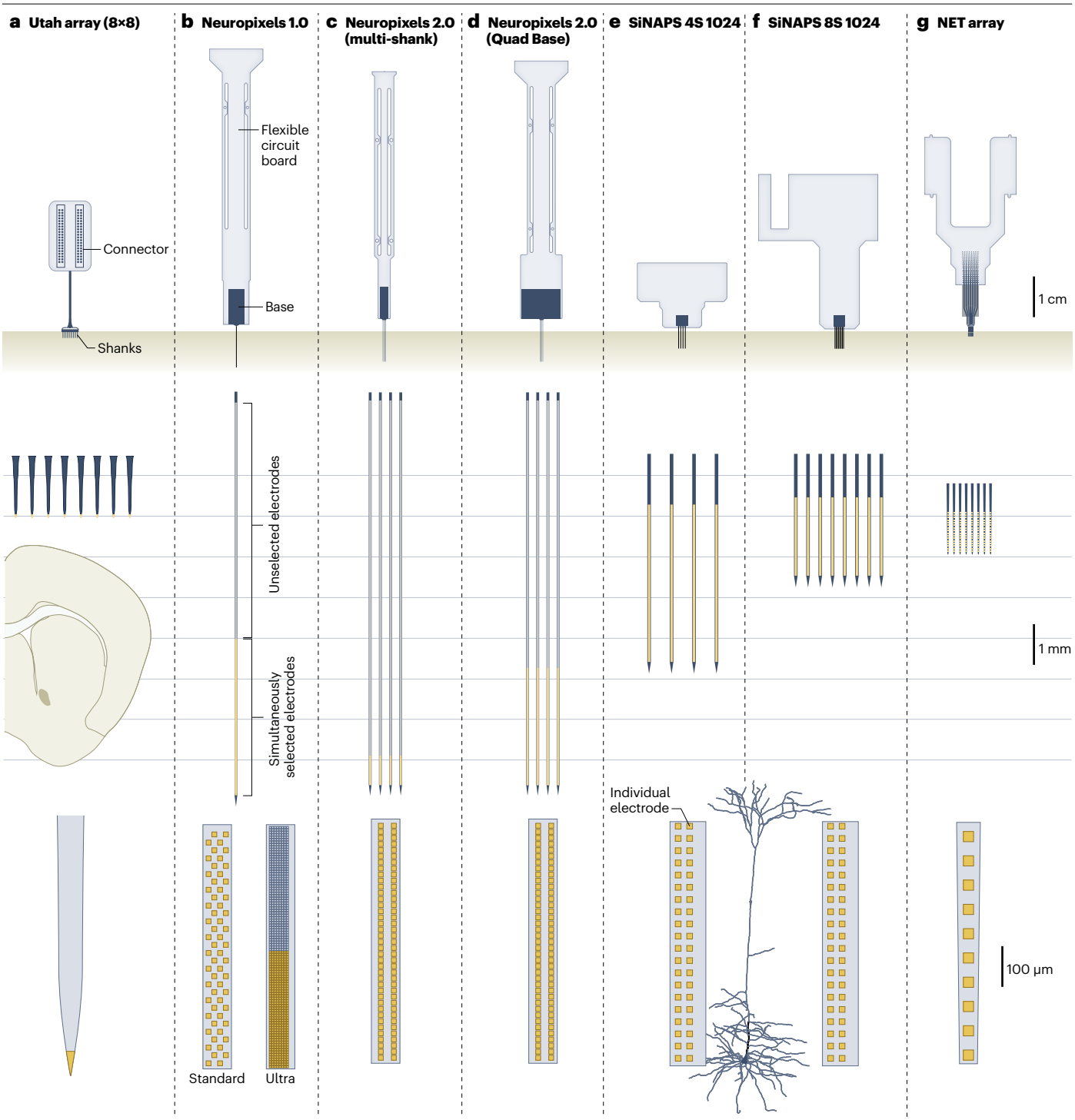

Fig. 3 | Example devices for large-scale electrophysiology. a–g, Top panels, overall package for seven example devices capable of large-scale electrophysiology (excluding headstage modules): Utah array (based on information from the Blackrock Neurotech website) (panel **a**); Neuropixels 1.0, including both 'standard' and 'ultra' electrode layouts (based on information from ref. 119 and the Neuropixels website) (panel **b**); Neuropixels 2.0 multi-shank (based on information from ref. 103 and the Neuropixels website) (panel **c**); Neuropixels 2.0 Quad Base (based on information from the Neuropixels website) (panel **d**); SiNAPS 4S 1024 (based on information from ref. 158 and the NeuroNexus website) (panel **e**); SiNAPS 8S 1024 (based on information from ref. 158 and the Plexon website) (panel **f**); and NET array (based on information from ref. 168) (panel **g**). The middle panels show the shank geometry for these devices. Yellow shading indicates the span of electrodes that can be read out simultaneously, grey indicates unselected electrodes and black indicates regions without electrodes. Mouse brain slice included for scale comparison. Lower panels, close-ups of individual shanks for these devices, with electrodes represented as gold squares (lower panels). Dendritic arbor of a mouse layer 5 cortical pyramidal cell included for scale comparison.

package and 10 mm shank length make it straightforward to insert multiple devices in the same subject and have enabled publications demonstrating simultaneous readout from 1,152 (ref. 12), 3,072 (ref. 67), 2,304 (refs. 15,120) and 1,536 (refs. 121,122) channels in head-fixed mice, and from 1,536 (ref. 123) or (as reported in a recent preprint) 3,072 (ref. 124) channels chronically implanted in the rat brain. As evidence of the relative ease of adapting these probes to novel preparations, Neuropixels 1.0 have now been used in a wide range of non-rodent species, including humans[125,126], macaques[127–131], marmosets[132], tree shrews[133], ferrets[134], bats[135], lizards[136], fish[55,137–139], birds[140,141] and cephalopods[142]. In the most well-studied systems, there have been numerous successful replications. For example, at least 14 laboratories have performed successful recordings with Neuropixels in rats in brain regions including the frontal cortex, hippocampus and brainstem[10,119,123,143–153].

Neuropixels 2.0 increases the number of electrodes per shank to 1,260 and introduces a four-shank probe[103] (Fig. 3c). Although each Neuropixels 2.0 probe contains more than 5,000 independent recording sites, simultaneous readout remains limited to 384 channels per probe. Neuropixels 2.0 probes have been used to record 1,536 channels from brain structures connected to the mouse anterolateral motor cortex during a delayed-choice task[13]. Furthermore, a recent preprint has reported recordings from 2,304 channels via a chronic implant in mice[154]. Additional Neuropixels variants include Neuropixels NHP, optimized for deep brain recordings in non-human primates[155], and Neuropixels Ultra, which has ten times the recording site density of Neuropixels 1.0 (ref. 55). Neuropixels Quad Base, a recent variant of Neuropixels 2.0 that can read out 384 channels on each of four shanks (Fig. 3d), promises to make 1,000+ channel recordings even more routine (see the Neuropixels website for more information).

The SiNAPS probe, another type of CMOS electrode array, originally allowed simultaneous readout of signals from up to 512 electrodes on a shank 88 µm wide[156]. Unlike Neuropixels probes, SiNAPS probes integrate an amplifier beneath each electrode, greatly reducing the amount of circuitry that must be located outside the shank. As a result, the electronics beyond the probe shank occupy only ~1 mm × 2 mm, providing a more compact packaging footprint[157]. SiNAPS probes are now available in four-shank (Fig. 3e) or eight-shank (Fig. 3f) configurations, each capable of recording from 1,024 electrodes simultaneously[158]. The eight-shank version, which samples spikes over an approximately 2 mm x 2 mm region of tissue, has proven effective for studying interactions across the CA1, CA3 and dentate gyrus (DG) subfields of the mouse hippocampus[159–162]. Scaling up channel counts even further by implanting multiple SiNAPS in the same subject has now been achieved in non-human primates, as reported in a recent preprint[163].

Devices in the 'Michigan' lineage have also been updated by making the shanks more flexible[62]. By depositing electrodes on a flexible substrate, such as polyimide, the shanks are more likely to move with the tissue, reducing issues caused by brain movements. These flexible substrates, which can be as thin as 1 µm, are thought to be better suited for long-term recordings than stiff electrodes[164,165] and a recent preprint has suggested that they may reduce relative motion between the probe and brain[166]; however, their implantation is complicated by their lack of rigidity and a stiffer guide is typically required for insertion. Similar to other passive probes, scaling of flexible shanks can be achieved by stacking smaller modules together, which has enabled 1,000+ channel recordings in rats[167,168] (Fig. 3g). Thus far, it has not been possible to combine CMOS fabrication (and the solution it provides to the connectorization problem) with these flexible materials. However, hybrid integration strategies, in which flexible probes are fabricated separately and then bonded to CMOS readout electronics via flip-chip or self-assembly techniques, offer potential pathways to robust scaling[169–172]. Other progress on the development of electrode arrays with flexible shanks has been reviewed in more detail elsewhere[62,173,174].

An alternative approach, which has evolved in parallel to the two lineages described above, is twisted wire tetrodes, with four electrodes per bundle[175]. Arrays of these independently movable tetrodes are particularly well suited for recording from the pyramidal cell layer of the rodent hippocampus, as the electrodes can be adjusted to follow the contours of this structure[176]. However, the size of these arrays has been limited to 16 tetrodes in a mouse (64 channels) and 64 tetrodes in a rat (256 channels)[177,178]. Owing to connectorization challenges and the extensive manual labour required for fabrication, further scaling of this approach is unlikely.

The original Utah and Michigan arrays had a great impact on the neuroscience community not only because of their device characteristics but also because of their wide dissemination. Of all the 1,000+ channel technologies discussed above, only Neuropixels have so far been widely disseminated. This highlights the critical importance of usability and accessibility in driving adoption. Ultimately, advancing neural recording technologies requires more than just improving specifications; it demands careful attention to system integration, implantation protocols and scalable manufacturing (Box 1).

Fixtures for multi-probe recordings

For electrophysiological probes with sufficiently small package sizes, the most efficient route to scaling up the total number of channels and brain regions per experiment is to insert multiple probes in parallel. The ideal device for multi-probe recordings should have a long shank and a narrow base, to minimize the probability of collisions between adjacent probes. Multi-probe recordings can either be performed acutely, with the electrodes temporarily inserted during the recording session, or chronically, with the electrodes permanently implanted in the brain.

The fixtures used to hold each probe have a major impact on both scalability and ease of use. Fixtures for acute recordings must be sufficiently compact to allow dense insertions and avoid interfering with other components of the electrophysiology rig. They should be adjustable, ideally via sliding mounts, to allow probe angles to be fine-tuned for different target regions. They must allow clear visibility of the probes and brain during the experiment, via either a stereomicroscope or machine vision cameras with long-working-distance lenses. Finally, it must be possible to move the probes far away (10 cm or more) from the brain while the subject is being placed on the rig.

Chronic recordings aim to track the same neural populations over weeks or months, typically by recording for a few hours daily but potentially even by recording continuously over the same interval[179]. For chronic implants, probes with a low centre of gravity are favoured over the long, narrow profiles that are advantageous for acute recordings. However, long shanks remain critical for accessing deep structures (up to 6 mm deep in mice, 10 mm in rats). The entire implanted package should, as a rule of thumb, be below 10–20% of the subject's body weight. For example, a 3 g weight on the head has been shown to minimally affect the behaviours of mice in open arenas[180]. Using a thin, coaxial cable and a torque-free commutator can greatly improve animal mobility[181].

Although large-scale chronic recordings have traditionally been more feasible in rats (owing to their larger skulls), these have recently been achieved in mice as a result of advances in electrode technology

Box 1 | The Neuropixels ecosystem: a case study in neurotechnology adoption

Since their introduction, more than 15,000 Neuropixels probes have been shipped to more than 1,000 laboratories worldwide. This widespread adoption is due not solely to the technological merits of the device but also to a unique confluence of collaborative, manufacturing and community-driven factors that together form the 'Neuropixels ecosystem'.

The core technological innovation of Neuropixels was the monolithic integration of high-density recording sites with complementary metal-oxide semiconductor (CMOS) circuitry for amplification, digitization and multiplexing. This technological leap was made possible by a strategic and collaborative funding model. The Neuropixels consortium, a partnership between the Howard Hughes Medical Institute, the Allen Institute, the Wellcome Trust and the Gatsby Foundation, provided the large-scale, high-risk investment necessary for such an ambitious engineering project. This model allowed close collaboration between neuroscientists and engineers and, crucially, supported a partnership with IMEC, an industrial semiconductor foundry and research institute. This partnership enabled probe fabrication with a high-yield and reproducible manufacturing process, ensuring quality and scalability. The combination of amplification on-probe, obviating any need for an external amplifier system, with scalable manufacturing and an at-cost pricing model dramatically lowered the financial barrier to entry for this cutting-edge electrophysiology, democratizing access for a wide range of laboratories.

The success of Neuropixels was further cemented by its model of dissemination and community support. The consortium developed a robust ecosystem of free and open-source software for data acquisition and analysis, which was later complemented by extensive community contributions (Box 2). Furthermore, free training courses have been run yearly both at University College London and at the Allen Institute and University of Washington. The high level of adoption of Neuropixels is therefore a case study in how the combination of a disruptive technology, a strategic collaborative and funding structure, and a commitment to open-access tools and data can accelerate progress across an entire scientific field.

and implant design. To simplify the implantation process and allow probes to be reused, the probe can be mounted within a fixture optimized for chronic recordings (but successful stable long-term recordings with the probe directly attached to the skull have been demonstrated[119,124,182]). Many such fixtures exist[150,152,180,183,184], but only two have been used for 1,000+ channel recordings to date. In rats, recordings with recoverable fixtures from up to four probes (1,536 channels) have been demonstrated[123], and a recent preprint has reported that, in mice, up to six Neuropixels 2.0 probes (2,304 channels) have been used for chronic recordings[154] (although it should be noted that the mice were head-fixed during recording owing to the excessive weight of the headstages and cables). The field of chronic recording fixtures is advancing rapidly, with new large-scale implant designs expected to emerge soon. These developments will progress in tandem with ongoing improvements in probe miniaturization and channel density.

Surgical techniques

Large-scale electrophysiology necessitates removing a portion of the skull (craniotomy) to provide access to the brain. Minimizing tissue damage during the craniotomy is essential for ensuring high-quality recordings[43,185]. In most cases, the craniotomy should be accompanied by removal of the dura mater (durotomy) to ensure that probes can easily penetrate the brain, although this is optional in mice. Following the craniotomy, the brain must be protected up to and during the recording session, minimizing exposure to air. If the craniotomy is large, the brain must be stabilized during the experiment to prevent the neurons from moving relative to the recording electrodes.

With these considerations in mind, the most straightforward surgical technique for large-scale electrophysiology in rodents involves drilling an individual craniotomy for each probe[67]. These craniotomies are usually small (<500 µm in diameter), but micromachined plastic honeycomb inserts have proven effective for brain stabilization for larger craniotomies[12,14]. However, it is impractical to scale this method beyond approximately eight probes in mice, owing to their limited skull surface area, and the method carries a risk of brain damage due to drilling near the intended recording site. An alternative approach involves drilling a single large craniotomy (≥5 mm) followed by a durotomy, which allows multiple probes to be flexibly positioned inside the craniotomy[15,186]. Here, stabilization is achieved by attaching a laser-cut plastic window approximately 1 mm above the brain surface, and filling the gap with a mixture of agarose and artificial cerebrospinal fluid. The laser-cut windows can be customized for each mouse to align the holes for each probe with the targets. However, a drawback of this approach is that it permits only two recording sessions on consecutive days, owing to the declining health of the exposed brain[186]. Most recently, large-scale electrophysiology has been performed through 3D-printed skull caps that span nearly one full brain hemisphere, or a portion of two hemispheres[120]. This approach supports recordings in diverse configurations for extended periods and offers exceptional scalability, accommodating 20 or more insertion points with multiple angle options per site. The large craniotomy and durotomy take practice to perform reliably, but can potentially be simplified by using robot-assisted surgeries[187].

In macaques, surgical techniques and probe-mounting strategies differ substantially from those used in rodents. The most common approach for awake subjects involves affixing a recording chamber to the skull, which provides stable *X*/*Y* positioning and precise depth control (*Z* axis)[155]. These chambers enable repeated access to the same cortical regions across multiple sessions while maintaining sterility and mechanical stability. An alternative strategy uses multiple chronically implanted Utah arrays[110,111], which do not need to be reinserted in every session. As in rodents, the field is rapidly evolving.

With appropriate sterilization and surgical preparations, Neuropixels have been successfully adapted for use in humans[188,189]. In clinical contexts such as tumour resection or implantation of stimulating electrodes, these procedures provide a rare and invaluable opportunity to record extracellular action potentials from individual neurons in awake people. Neuropixels recordings in humans have already yielded important insights into the neural mechanisms underlying language production and comprehension[125,126,190]. To date, these probes appear to be extremely safe, with no reported complications arising

from insertion[191]. A recent preprint demonstrated the use of 45 mm Neuropixels NHP probes to record from the human hippocampus[192]. These probes are comparable in length with standard stereoelectroencephalography electrodes, but offer dramatically higher spatial resolution, with 4,416 recording contacts compared with roughly 10 for typical stereoelectroencephalography electrodes. Remaining challenges include managing pulsatile brain motion driven by the cardiac cycle[105], maintaining surgical sterility and minimizing electrical interference. Detailed protocols designed to address these issues have been published and are now available to the community[193].

Data quality and reproducibility

Spike sorting and preprocessing

Spike sorting is a critical step in interpreting the datasets that arise from large-scale electrophysiology recordings. To analyse the neural responses, it is first necessary to extract relevant information from the raw recorded voltage values. The goal of a spike sorting algorithm is to automatically determine the time and identity of every action potential present in the recording[194]. In this context, 'identity' only means that the spikes attributable to a single source in the extracellular space are labelled as being part of a distinct group. Other aspects of identity, such as the genetic cell type or morphological element giving rise to the waveforms, are considered below. A collection of extracellular events that were detected and grouped together are known as a 'unit'[35,195], and typically correspond to action potentials recorded from a neuron or neurite. The spike sorting algorithm achieves automatic detection and segregation into units on the basis of two key assumptions: that every voltage deflection produced by a unit will be identical in its spatial and temporal profile, and that each neuron's waveform is distinct from that of every other neuron.

The key challenges for spike sorting algorithms in the context of large-scale recordings are to scale to many channels with acceptable runtime and computational resources, and to accurately combine information across channels to optimize sorting. To scale appropriately, recent algorithms have taken advantage of GPU-accelerated computing and cross-channel dimensionality reduction techniques[196–198]. To combine information across channels effectively, two recent preprints have reported on the use of dense sampling to extract explicit estimations of spike location relative to the probe[199,200]. Other algorithms define the joint cross-channel features to be applied when detecting and clustering spikes[197,198].

Dozens of spike sorting algorithms have been developed and published, with more released on a regular basis[201–205]. It is beyond the scope of this Review to comprehensively compare their qualities[206]. To aid users in dealing with the overwhelming glut of available algorithms, the SpikeInterface package was developed[207], which allows at least 14 of these algorithms to be run on a given dataset by changing only a single line of code. This capability was recently used to show that a new algorithm, Kilosort4, substantially outperformed several comparison algorithms when run on synthetically generated ground truth datasets[197]. As a result, Kilosort is now the most commonly used spike sorting algorithm for Neuropixels data[12–15,208]. Nevertheless, the best algorithm may differ by probe and recording preparation and may depend on the metrics used to assess performance. Factors such as noise levels, species, brain region, behavioural state, recording site density and geometry, presence of artefacts and probe–brain stability may all influence spike sorting results, motivating the continued need for experimenters to carefully assess the results of algorithms on their own data and for algorithm developers to continue to strive for maximally generalizable approaches.

The field is fortunate to have a plethora of freely available spike sorting algorithms, but important challenges remain. One is ensuring reproducibility: whereas tools such as SpikeInterface are a step in the right direction, true reproducibility also requires tools that integrate with databases to track the provenance of all inputs and outputs of a processing pipeline, such as DataJoint[209] or Code Ocean[210]. Another challenge is scalability. The time needed to preprocess and spike sort data from a single Neuropixels probe exceeds the overall duration of the recording, making parallelization essential for timely analysis[206]. To avoid the burden of each laboratory maintaining its own high-performance computing cluster, cloud-based solutions are a logical path forward, but adoption has so far been limited[211–213]. Finally, the technical difficulty of carrying out large-scale electrophysiology recordings in which the true spike times are known (for example, via simultaneous intracellular sampling) means there are extremely scarce genuine ground truth data available for benchmarking or supervised training[39,214–216].

Given these challenges, it is critical that all spike sorting results are assessed with objective quality metrics[217]. This is also important because spike sorting algorithms perform their task imperfectly. The spatial arrangement of neurons around recording electrodes generates a continuous distribution of recorded waveform amplitudes, with ever-increasing numbers of waveforms at lower amplitudes. For any given electrode and recording location there will always be many neurons that fall near or just below the limits of high-quality isolation[39,218]. Accurately distinguishing the well-isolated neurons from poorly-isolated neurons is therefore critical for maximizing yield while preserving the ability to make accurate scientific conclusions free from confounds. Software packages such as phy enable the manual review of spike sorting outcomes and correction of errors on the basis of visual inspection[219], but manual curation is extremely time consuming and hinders reproducibility, as each annotator relies on subjective decisions.

To improve reproducibility, automatic quality metrics that seek to estimate false positive and false negative sorting errors may be used, either replacing or aiding the manual process. To estimate false positive errors, investigators have classically relied on the refractory period, a biophysical property of neurons preventing them from spiking twice in a brief window. If instances of doublet spikes with a time interval shorter than that window are observed, called 'refractory period violations', they can be taken as an indication that the spikes did not all originate from a single unit. By considering the number of observed refractory period violations and the firing rate of the unit, a putative false positive rate can be estimated[217]. However, this method assumes the independence of firing rates of nearby neurons[220]. In general, the firing of neurons is positively, although weakly, correlated with that of their neighbours[221–223], which will lead to under-estimates of the false positive rate. Another limitation is the assumption of a fixed and constant refractory period duration. A recent preprint reported that the observed refractory period durations of neurons differ substantially between brain regions and species[224], which may lead to overestimates or underestimates of the false positive rate. To maximize statistical power, estimate statistical reliability and avoid inaccurately excluding neurons with truly low false positive rates, the preprint introduced an algorithm that flexibly tests a range of refractory period durations[224]. Older approaches for determining false positive errors emphasized the separation of waveform shapes between units[225], but such approaches are not robust to recording instability, do not generalize well to high-dimensional waveforms and, generally,

are not directly interpretable as error rates. Overall, using refractory period violations to estimate false positive rates is the best available method for making this estimation. Similarly, estimates of false negative rates can be made in several ways. First, spike amplitudes can be examined in relation to the spike detection threshold to determine whether some spikes emitted by the neuron were likely to have fallen below the threshold and missed. This method assumes that the true distribution of amplitudes is Gaussian, which will be true when the recording is stable[217]. In the presence of instabilities, modified methods can be used[226,227]. Second, false negatives can be inferred from the 'presence ratio', which computes the proportion of a session in which a neuron has no spiking[207]. Although this method could errantly exclude neurons that have true pauses in their spiking and is sensitive to noise, it nevertheless provides a reproducible way to exclude units that may have substantial false negatives.

Interpretation of scientific conclusions may depend crucially on the nature and extent of spike sorting errors, and it is therefore critical to consider these errors even at the final stages of analyses. For example, if authors intend to draw a conclusion about mixed selectivity, in which individual neurons represent multiple properties rather than a single variable, false positive errors could be fatal: they could lead to the appearance of mixed selectivity where there is none. Or, if authors intend to argue that absolute firing rates differ between their data and a published result in the literature, then false negative errors could confound, leading to lower estimated firing rates than the true values. It is tempting, in the face of such considerations, to decide only to accept 'perfect' units with minimal or unmeasurable error rates. But for many analyses this would be a mistake: a strength of such large-scale recordings is in accessing high-dimensional populations, and, for many analyses, errors of these kinds are acceptable or irrelevant, especially when moderate in magnitude. Indeed, multiple authors have argued that spike sorting can be omitted entirely for analyses such as decoding or dimensionality reduction[129,228,229]. Therefore, we advocate a different solution to the problem: do not approach analysis by first 'completing' spike sorting and then forgetting it entirely and assuming the data are perfect. Instead, apply reasonable quality metrics, but keep the values of these quality metrics to use in validating scientific conclusions. For example, after understanding the scientific claim to be made and its potential dependence on false positive or negative errors, control analyses could either subselect neurons or plot the effect size as a function of metric value[230].

Reproducibility

For findings to accumulate into lasting knowledge, they must be reproducible across laboratories, experimenters and time. In comparison with many physiological measurements, electrophysiological recordings stand out in this regard: spike trains are fundamentally discrete and binary, making them inherently more reproducible than analogue signals. When electrodes are placed in the same brain region under comparable conditions, the resulting activity patterns are remarkably consistent; for example, place fields in the CA1 region of the hippocampus and orientation tuning curves from the primary visual cortex (VIS) have been reliably observed for more than 50 years[231,232]. Nevertheless, as large-scale recordings generate ever greater volumes of data, we should aspire to a higher standard of reproducibility. This requires careful control of at least four factors: signal quality, inclusion criteria, anatomical localization and behavioural state.

Reproducible signal quality has benefited from the widespread adoption of Neuropixels probes, whose industrially scaled production has led to standardized recording characteristics, including site geometry and noise levels across devices. This contrasts with earlier approaches, such as tetrode microdrives, which had inherently high device-to-device and site-to-site variability due to their reliance on hand fabrication. In parallel, freely available training courses held on multiple continents, accompanied by openly shared instructional materials, have accelerated the dissemination of best practices (Box 1). Still, careful attention must be paid to grounding and electrical isolation of the recording apparatus to prevent contamination of signals by electrical noise. Beyond hardware, a robust ecosystem of free and open-source software has developed to support all stages of large-scale electrophysiology, enhancing reproducibility through standardization and openness of data pipelines and other software-dependent experimental steps (Box 2).

Reproducibility in electrophysiological analysis depends on transparent and consistent inclusion criteria, in terms of which sessions are retained and which neurons are analysed. Explicitly reporting these criteria is essential, as even subtle differences in quality metric thresholds or behavioural performance filters can lead to divergent results. Encouragingly, when identical spike sorting pipelines and inclusion criteria were applied to three independent electrophysiological surveys, there were similar yields of well-isolated neurons in the cortex, hippocampus and thalamus[233] (Fig. 4a). To test experimental reproducibility in a more explicit way, the International Brain Laboratory (IBL) established tightly controlled experimental apparatuses and protocols in 10 laboratories and performed 121 repetitions of an experiment targeting the same location in the brain. In this setting, detectable differences in experimental outcomes between laboratories were largely absent, particularly when considering more robust types of analysis and excluding recordings that deviated too far from the intended recording location (Fig. 4b). The investigators developed a set of recommendations, called the Recording Inclusion Guidelines for Optimizing Reproducibility (RIGOR), that can be applied by other investigators[233].

Even when targeting the same nominal brain region, substantial variability in spiking properties can arise from subtle differences in electrode placement. The dense sampling afforded by Neuropixels probes has revealed continuous gradients of function within many structures, showing that reproducibility often depends on targeting specific subregions rather than broad anatomical labels[13,234,235] (Fig. 4c–e). Given the variability in electrode targeting based on stereotaxic coordinates, differences in probe locations of only a few hundred microns may have a substantial impact on observed functional properties. Traditionally, electrophysiologists identified target coordinates using brain atlases developed from a single perfused brain[236] and verified recording locations with small electrolytic lesions visualized in ex vivo brain slices. Large-scale recordings demand higher fidelity, both for insertion planning and for electrode track reconstruction. MRI scans, which more accurately reflect the 3D structure of the brain in vivo[237–241], can be incorporated into software packages that simulate the geometry of multi-probe insertions during the experimental planning phase[242]. Electrode localization and assignment to brain regions involves coating the shanks with fluorescent dye and, subsequently, imaging brains with optical projection tomography, light-sheet imaging or serial section two-photon imaging. The imaged volume can be automatically aligned to a reference atlas and the probe track localized to identify the brain regions through which the probe passed. As a final step, the electrophysiological features observed along the probe can be used to refine the estimated depth of the probe, and to

account for variable scaling of individual brains[12,243]. Together, this process results in fast and accurate resolution of the locations of large numbers of recording sites throughout the brain. In the future, the availability of large sets of recordings from across many brain locations[19] may enable the automated identification of probe location based on electrophysiological features alone.

Box 2 | Free and open-source software from data acquisition to analysis

Developing and publishing free, open-source software for the scientific community is a crucial and often thankless task, typically minimally supported by funders, hiring committees and award panels. Moreover, development and publication are only the very beginning of the work for any tool that seeks to have long-term impact. User support, bug-fixing, development of training materials and outreach all cost countless hours of expert time. The in vivo electrophysiology community is large enough for these to be full-time jobs but generally not large enough for the formation of profitable software companies. Nevertheless, through various funding sources, institutions and individuals generous with their resources and time, an extensive ecosystem supports fully free and open-source software for every step from data acquisition to figure production. A sample of these are recognized in the Table.

Software	Financial support	Link
Data acquisition software		
Open Ephys GUI[312]	Massachusetts Institute of Technology (MIT), US National Institutes of Health (NIH), Open Ephys, Inc. and Allen Institute	https://open-ephys.org/gui
Bonsai[313]	Bonsai Foundation community interest company (CIC), Champalimaud Foundation, NeuroGEARS, Open Ephys, Inc., Sainsbury Wellcome Centre and Allen Institute	https://bonsai-rx.org/
SpikeGLX	Janelia Research Campus (Howard Hughes Medical Institute), Wellcome Trust and NIH	http://billkarsh.github.io/SpikeGLX/
Spike sorting software		
Kilosort[197]	Wellcome Trust and Janelia Research Campus (Howard Hughes Medical Institute)	https://github.com/MouseLand/Kilosort
SpyKING Circus[198]	Agence Nationale de la Recherche	https://github.com/spyking-circus/spyking-circus
MountainSort[314]	NIH, Simons Foundation and Howard Hughes Medical Institute	https://github.com/flatironinstitute/mountainsort5
Software for spike sorting review		
Phy[219]	Wellcome Trust and Gatsby Charitable Foundation	https://github.com/cortex-lab/phy
SortingView	Flatiron Institute (Simons Foundation)	https://github.com/magland/sortingview
Sorting pipelines and quality metrics		
ecephys_spike_sorting	Allen Institute and Janelia Research Campus (Howard Hughes Medical Institute)	https://github.com/AllenInstitute/ecephys_spike_sorting
Bombcell[227]	Wellcome Trust, Mathworks and Schmidt Science Fellows in partnership with the Rhodes Trust	https://github.com/Julie-Fabre/bombcell
SpikeInterface[207]	Wellcome Trust, Norwegian Ministry of Education and Research, and Allen Institute	https://spikeinterface.readthedocs.io/
UnitRefine[315]	UKRI Biotechnology and Biological Sciences Research Council, Helmholtz Association and North Rhine-Westphalia through the iBehave initiative	https://github.com/anoushkajain/UnitRefine
Software for electrode targeting and histology alignment		
Pinpoint[242]	Wellcome Trust, Simons Foundation and NIH	https://github.com/VirtualBrainLab/Pinpoint
IBL Alignment GUI[243]	Wellcome Trust and Simons Foundation	https://github.com/int-brain-lab/ibl-alignment-gui
HERBS[316]	Research Council of Norway	https://github.com/Whitlock-Group/HERBS
AP_histology[317]	Wellcome Trust and Royal Society	https://github.com/petersaj/AP_histology
Analysis software		
Elephant[318]	EU Horizon 2020 and Human Brain Project	https://neuralensemble.org/elephant/
Pynapple[319]	Canadian Institutes of Health Research and Simons Foundation	https://pynapple.org/
Tool index		
Awesome Neuropixels	None	https://github.com/Julie-Fabre/awesome_neuropixels

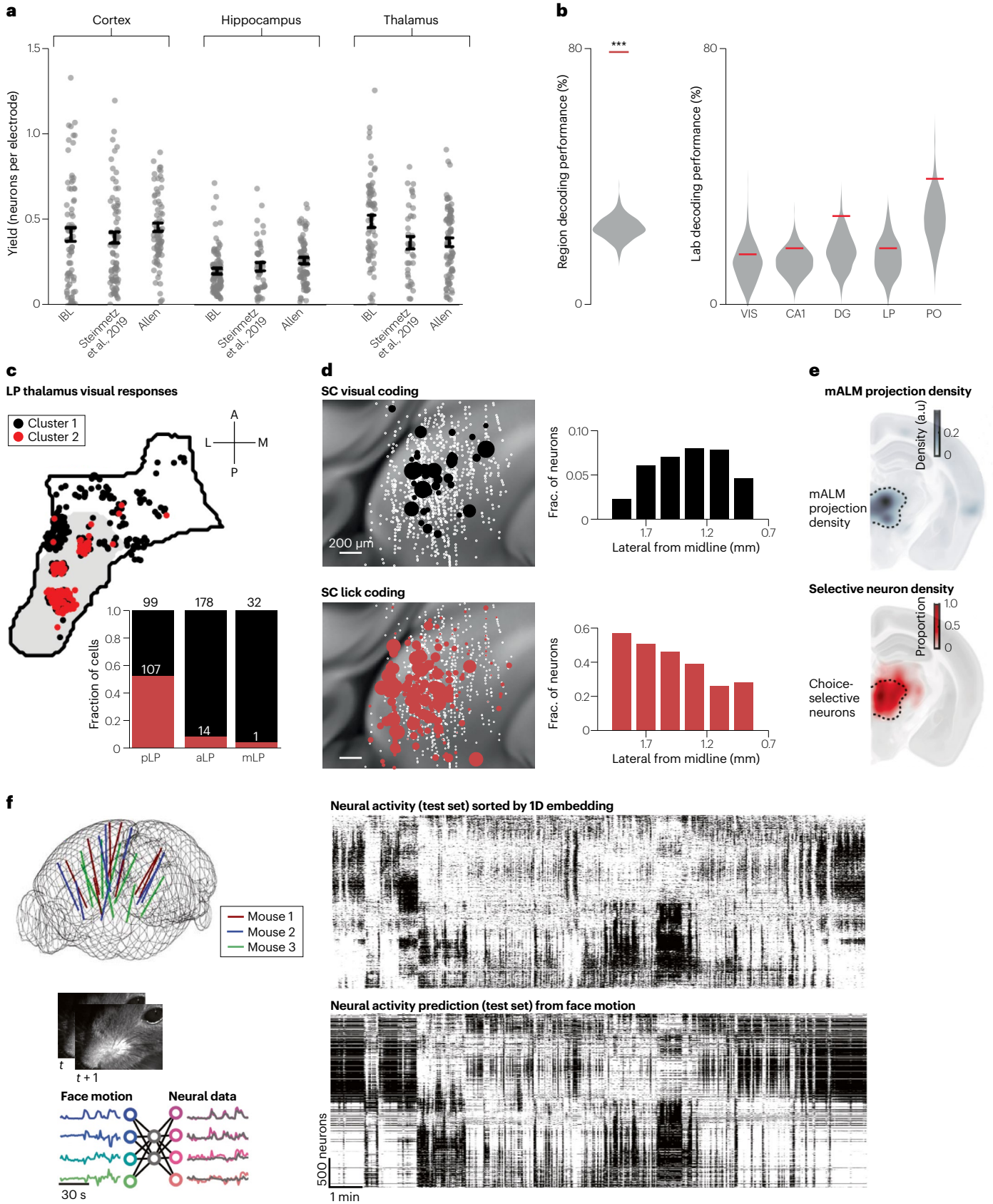
a
Cortex
Hippocampus
Thalamus
Yield (neurons per electrode)
1.5
1.0
0.5
0
IBL
Steinmetz et al., 2019
Allen
b
***
Region decoding performance (%)
Lab decoding performance (%)
80
0
VIS
CA1
DG
LP
PO
c
LP thalamus visual responses
Cluster 1
Cluster 2
A
L
M
P
Fraction of cells
99
178
32
107
14
1
pLP
aLP
mLP
d
SC visual coding
200 µm
Frac. of neurons
0.10
0.05
0
1.7
1.2
0.7
Lateral from midline (mm)
SC lick coding
0.6
0.4
0.2
e
mALM projection density
Density (a.u)
mALM projection density
Selective neuron density
Proportion
1.0
0.5
Choice-selective neurons
f
Mouse 1
Mouse 2
Mouse 3
t
t + 1
Face motion
Neural data
30 s
Neural activity (test set) sorted by 1D embedding
Neural activity prediction (test set) from face motion
500 neurons
1 min

Fig. 4 | Reproducibility of large-scale electrophysiological measurements. **a**, Average yield of sorted neurons from the mouse brain is reproduced across three independent datasets, but is highly variable from session to session[233]. Datasets are from the International Brain Laboratory (IBL)[233], Steinmetz et al.[12] and the Allen Institute[15]. **b**, A random forest classifier trained on data from the IBL can identify brain regions well above chance (left panel, $^{***}P < 0.001$), but fails to decode the laboratory identity for any region (right panel)[233]. Distribution based on shuffled samples is shown (grey), with the actual decoder performance indicated (red line). **c**, Visual responses in mouse lateral posterior nucleus of the thalamus (LP) depend on the anatomical location within this structure[234]. Neurons in the posterior LP (pLP),which receives dense inputs from the superior colliculus (SC), form one response cluster (red), whereas neurons in the medial and anterior LP (mLP/aLP), which receive dense visual cortical inputs, form a distinct cluster (black). Without precise alignment of neurons to reconstructed electrode tracks, LP responses would appear substantially more heterogeneous. **d**, Neurons in the mouse SC display a medial–lateral gradient of selectivity for vision-related (black) and movement-related (red) stimuli. Consequently, shifting electrodes by only a few hundred micrometres could bias interpretation of the SC as either a sensory-dominated or motor-dominated structure[235]. **e**, During the delay period in a cued licking task, choice-selective neurons in mouse thalamus overlap with projections from the medial anterolateral motor cortex (mALM)[13], illustrating how targeting of projection-defined circuits is required to capture functional differences. **f**, Motor behaviours (such as whisking and eye movements) strongly correlate with neural activity, so idiosyncratic features of the subject's state and behaviour from session to session will drive substantial across-session variability. Large-scale Neuropixels recordings were performed, yielding a matrix of neuronal activity across neurons and time (upper greyscale image). Simultaneous video of the mouse face was recorded and a reduced-rank predictive model was fit to predict the neural data. The resulting prediction of neural activity on held-out, test set data (lower greyscale image) captured significant parts of the true test set data[67]. CA1, cornu ammonis 1; DG, dentate gyrus; PO, posterior nucleus of the thalamus; VIS, visual cortex. Panels **a** and **b** are adapted from ref. 233, CC BY 4.0 (https://creativecommons.org/licenses/by/4.0/). Panel **c** is adapted with permission from ref. 234, Elsevier. Panel **d** is adapted from ref. 235, Springer Nature Ltd. Panel **e** is adapted from ref. 13, CC BY 4.0 (https://creativecommons.org/licenses/by/4.0/). Panel **f** is adapted with permission from ref. 67, AAAS.

Large-scale recordings have made it increasingly clear that an important source of variability in electrophysiological activity arises from its tight coupling to an animal's behavioural state[67,244,245]. Variables such as locomotion, pupil diameter and whisking can be decoded from neural activity in nearly any brain region, illustrating the pervasiveness of state-dependent modulation (Fig. 4f). Reproducible recordings therefore require careful monitoring of the behavioural state through video, inertial sensors or other continuous measurements so that neural dynamics can be related to ongoing behaviour. The shared dependence on aspects of state such as arousal, engagement and motor patterns[12,19,67,244,246] necessitates careful avoidance of statistical methods that would assume independence of simultaneously recorded neurons. Finally, the diversity of coding properties across neurons underscores the value of sampling large populations with high-density probes, enabling enhanced accuracy in estimation of population activity on individual trials.

Data sharing to maximize impact

When thousands of neurons and dozens of brain regions are recorded in parallel, it is unlikely that the original experimenters will exhaust all of the possible analyses. With data storage services capable of hosting and transmitting terabytes of data, these datasets can be shared in either raw or preprocessed forms. This type of large-scale data sharing is a relatively novel development, with the core principles for modern data sharing, the 'FAIR' conventions, only established in 2016 (ref. 247).

Neuroscience data sharing follows in the footsteps of the field of genomics but faces different challenges, including the variety of underlying data types and the dependence of measurements on experimental manipulations[248]. The history of neuroscientific data sharing has been reviewed elsewhere[249], with major landmarks for neurophysiology including the establishment of the CRCNS (Collaborative Research in Computational Neuroscience) database in 2008 (ref. 250), the development of the Neurodata Without Borders sharing format in 2015 (ref. 251), the introduction of DANDI (Distributed Archives for Neurophysiology Data Integration) in 2019 (ref. 252) and the launch of the EBRAINS data sharing infrastructure in 2020 (ref. 253). The increasing prevalence of data sharing in large-scale electrophysiology has been exemplified by the availability of major datasets from the Allen Institute[15], the IBL[19] and multiple individual research groups (Fig. 5). Large, openly shared datasets have also been released from studies of other species including rats[208] and non-human primates[254].

With the availability of these datasets, investigators can answer specific questions that may not have been the focus of the original data acquisition without new data collection. Although false positive results may become more likely with extensive reanalysis of the same dataset, typically the analyses are sufficiently orthogonal to avoid this. For example, investigators have relied on open datasets to study the timescales of neural activity across regions[23,25], the variability of spiking responses[255] and the dimensionality of neural representations[256,257]. An open dataset designed to study the mouse visual system has revealed a surprising number of fundamental insights into the function of the hippocampus[258–261]. In this way, these datasets function similarly to public resources, and the laboratories collecting them are similar to astronomical observatories — facilities that use specialized infrastructure and personnel to collect large-scale data and make them available for the community to mine[262,263].

This system has multiple benefits. First, new ideas can quickly be confirmed or rejected in multiple distinct datasets. Second, individual investigators have less need to simultaneously develop expertise in both experimental and theoretical skills, as the data may already exist to answer their questions. Third, by accessing the same datasets, the community may more easily find consensus on the comparison between ideas, instead of arriving at competing answers by using different methods on different datasets. However, many scientific questions will require targeted experimental manipulations and specific approaches that must be carefully designed at the experimental level, so data sharing by centralized observatories cannot become the only model. Moreover, as dataset sizes and sharing practices expand, the costs and burden of hosting these datasets will correspondingly grow, underscoring the need for appropriate data compression strategies[264]. Despite these limitations, the benefits of data sharing are apparent and the increasing prevalence of this practice is welcome.

Future advances

Devices for large-scale electrophysiology have evolved rapidly, but there is still plenty of opportunity for further improvement. Three

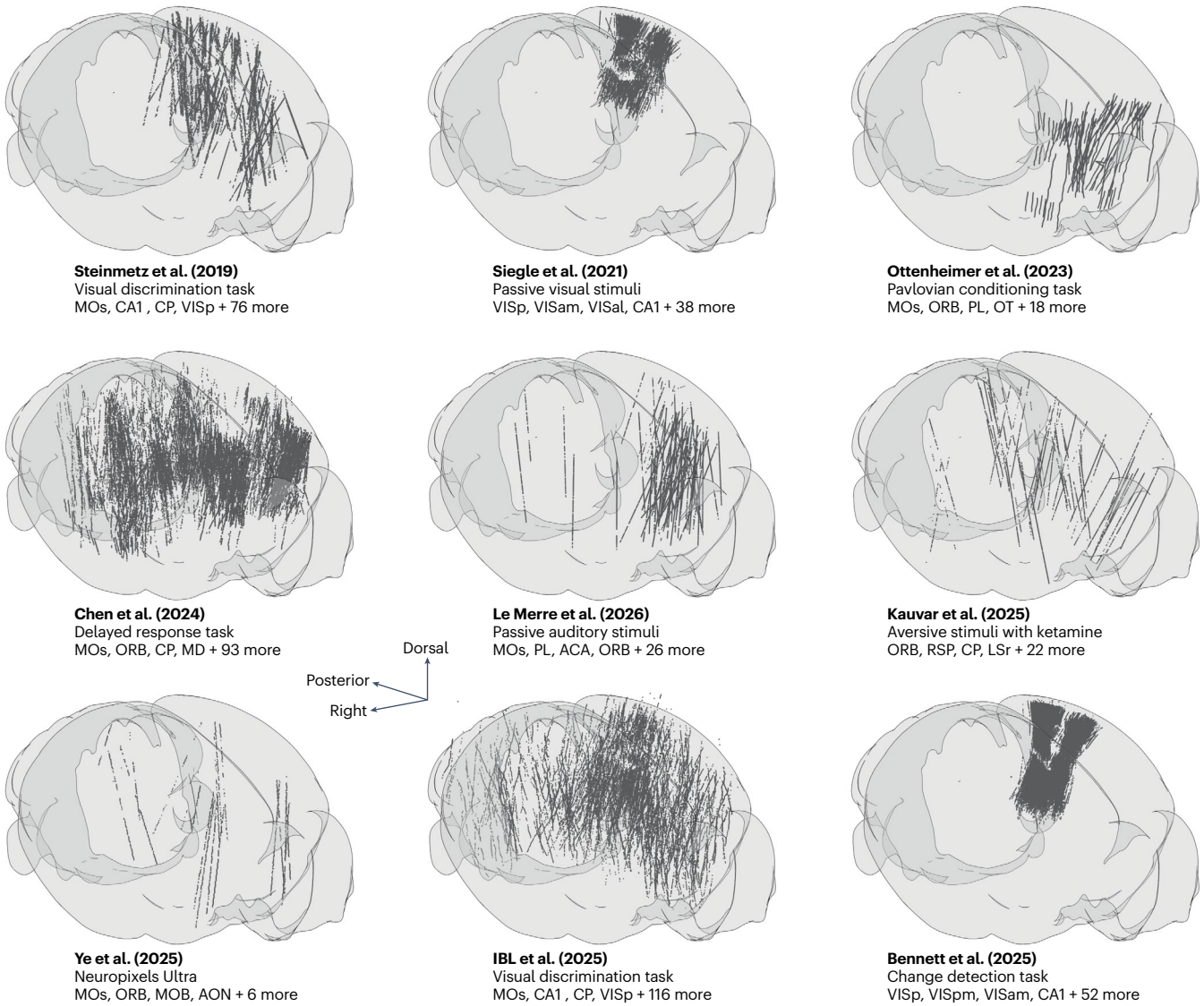

Fig. 5 | Large-scale, open datasets available for studying distributed spiking activity. New recording technologies have enabled activity surveys spanning many brain regions, and the resulting datasets are increasingly shared in standardized formats to facilitate new analyses. Within a dataset, spiking activity can be compared across regions under a common paradigm, whereas overlapping coverage across datasets enables cross-condition comparisons of the same regions. Subpanels were generated by downloading publicly released data from nine mouse studies and extracting each recorded neuron's position in the Common Coordinate Framework (CCF)[307], which were rendered as black dots inside a 3D brain volume[308]. Each study is identified by its lead authors, behavioural paradigm and four representative brain regions. The corresponding publications, from left to right and top to bottom, are refs. 12,15,309,13,18,310,55,19,311. ACA, anterior cingulate area; AON, accessory olfactory nucleus; CP, caudoputamen; IBL, International Brain Laboratory; LSr, rostral lateral septal nucleus; MD, mediodorsal nucleus of thalamus; MOB, main olfactory bulb; MOs, secondary motor area; ORB, orbital area; OT, olfactory tubercle; PL, prelimbic area; RSP, retrosplenial area; VISal, anterolateral visual area; VISam, anteromedial visual area; VISp, primary visual area; VISpm, posteromedial visual area.

areas where additional development would be highly beneficial relate to scaling up channel counts, integrating tools for circuit manipulations and extending the duration of stable recordings.

Scaling up channel counts

For passive probe designs, scaling is constrained by the minimum feature size of the fabrication process, which determines how densely traces can be routed on the shank. The primary approach to increasing electrode counts in passive devices without increasing the shank width has been to stack multiple probes together[117,118,168]. Although this strategy is feasible in larger animals, it is impractical in mice because of strict limits on implant size and weight. Another avenue for boosting the electrode count is to add features on both faces of the shank[265] or to the four faces of a square-profile shank[266]. Dual-sided probes are now commercially available and yielding important insights[267,268]. However, as electrode densities increase, passive probes remain dependent on external amplification via bulky interconnects, imposing practical limits on scalability.

Active CMOS-based probe designs with integrated electronics offer greater potential for miniaturization by substantially reducing the external connections required to read out data from the same number of electrodes. The semiconductor industry faces strong pressure to develop progressively smaller CMOS feature sizes, enabling increasingly complex circuitry within the same physical area. Neuropixels 1.0 probes were fabricated using a 130 nm process introduced in the early 2000s, which was used to create processors for the original Microsoft Xbox. Neuropixels devices currently under development use a 55 nm process, similar to that used in the Sony PlayStation 3, which enables a fourfold increase in channel count while preserving the same probe dimensions[269]. In principle, even smaller process nodes could be adopted; state-of-the-art consumer electronics are now manufactured at 3 nm, with sub-nanometre technologies on the horizon. However, shrinking feature sizes yield diminishing returns for low-noise analogue applications (such as detecting spikes). Manufacturing costs rise steeply, and analogue performance can degrade owing to increased gate leakage current, noise and device variability[270].

In acute experiments, channel counts can be increased by implanting more probes, provided that the probe bases and interconnect cables do not interfere with one another. In chronic experiments, simply adding more devices is less advantageous because of the limited space for long-term implants and the added burden on the animal. Instead, increasing the number of shanks per device and miniaturizing the readout electronics in the base offers a more effective path to higher channel counts. Current development efforts often focus on probes that can be used in both acute and chronic contexts, but the requirements for chronic recordings are distinct. Dedicated CMOS probe designs optimized specifically for chronic use could therefore have substantial impact and are likely to be in high demand[271].

Integrating circuit manipulations

Integrating precise circuit manipulations with large-scale electrophysiology is another area of active development. Most neural circuit manipulations are not done in conjunction with real-time feedback about ongoing activity, which can hide paradoxical or off-target effects[272–274]. Achieving tight temporal and spatial coupling of stimulation and recording is therefore essential to interrogate and control neural circuits more effectively.

A variety of devices have demonstrated parallel light emission and recording capabilities[275–279], but developing such devices with sufficiently high channel counts to meet our definition of 'large scale' has proven challenging. However, a recent study reported the development of Neuropixels Opto probes, in which light emission is integrated alongside electrodes at densities comparable with Neuropixels 1.0 (ref. 280). These devices enable spatially restricted circuit manipulations (on the order of ~200 µm) and permit optotagging of sub-populations expressing light-sensitive opsins. Integration of light emission with large-scale recording devices has also been demonstrated by attaching optical fibres to SiNAPS probes[281]. Optotagging has been successfully used to identify diverse cell types in vivo[90,282–284], yet remains underutilized across the field as a whole. Major challenges that limit its use include the need to achieve genetic access to specific cell types, minimize light-induced artefacts and ensure precise spatial overlap between recording and illumination sites. Neuropixels Opto addresses the latter two limitations by restricting light delivery to a small area adjacent to the probe shank while maintaining high-density sampling. Developing practical tools for optotagging in large-scale electrophysiology is essential, as this technique remains the gold standard for linking spike trains to transcriptomically defined cell types. Machine learning tools for automated cell-type identification based on electrophysiological features show increasing promise[92,285–287]. However, their success ultimately depends on the availability of ground truth training datasets obtained via devices capable of substantially increasing the throughput of optotagging across diverse brain regions and cell classes.

Electrical stimulation remains an indispensable method for perturbing neural activity, particularly in species or contexts where optogenetic methods are impractical[288]. With passive probes, current can be externally injected through any recording site[289,290]. By contrast, electrical stimulation through CMOS probes requires on-chip high-voltage driver circuits fabricated in specialized technology nodes. To minimize electrical interference during periods of stimulation, these devices, which have primarily been used for in vitro applications, also demand dedicated artefact suppression mechanisms and careful circuit design[291].

Chemical neuromodulation via integrated microfluidic channels provides an additional avenue for circuit manipulation. For instance, local infusion of AMPA receptor antagonists can transiently suppress excitatory synaptic transmission, enabling validation of optotagging results by confirming that light-evoked spikes arise from direct, rather than synaptic, activation[292]. Similarly, focal delivery of GABA receptor agonists allows reversible silencing of neuronal populations[293]. Passive probes incorporating nanodialysis have been demonstrated[294], permitting both localized drug delivery and extracellular sampling. Multifunctional probes combining electrophysiology, nanophotonic waveguides and microfluidic channels were recently developed[295,296]. Although chemical manipulation has yet to be integrated with active CMOS probes, doing so could substantially expand our ability to link cellular mechanisms to system-level dynamics.

Extending recording durations

Increasing the duration of electrophysiological recordings is essential for studying neural dynamics across longer relevant timescales, such as sleep–wake cycles[136] and learning over days of experience[154]. Conventional wisdom favours flexible electrode materials for long-term use[62]. However, more direct comparisons between rigid and flexible electrodes in similar brain regions and experimental conditions are needed to establish whether flexibility confers consistent advantages for chronic recording performance[165,297]. Increasing shank compliance (while maintaining stiffness) would also substantially extend the device lifespan by reducing the probability of breakage.

Beyond electrode materials, additional challenges limit the duration of chronic recordings. Head-mounted devices must remain powered at all times, although recent progress towards battery-powered data loggers for Neuropixels has been encouraging. An SD-card-based data logger has enabled wireless recordings in freely moving rats[184,298] and bats[135]. Wireless data transmission and power delivery would further extend the recording duration, but currently available systems support only dozens of channels, rather than thousands[299–301]. Power delivered over a tether can, in principle, support unlimited recording durations, although conventional tethers often restrict movement because of their bulk or twisting over time. This has been addressed by the ONIX platform[181], which uses a commutator linked to a head-mounted tracking unit to actively counteract tether twisting. Finally, spike sorting over long durations remains a major obstacle; reliably tracking individual neurons and assessing sorting accuracy over time are active areas of investigation[302–304]. The ability to track neurons successfully is notably enhanced by densely spaced electrode arrays

Glossary

Calcium imaging
An optical imaging technique that uses fluorescent calcium indicators to detect neural activity, typically using two-photon imaging for neuronal or sub-neuronal spatial resolution but with temporal resolution limited by indicator kinetics and imaging rate.

Complementary metal-oxide semiconductor
(CMOS). A semiconductor fabrication technology that enables the monolithic integration of high-density recording sites with on-chip amplification, digitization and multiplexing circuitry, as used in Neuropixels probes.

Dimensionality reduction
A set of computational techniques that compress high-dimensional neural data (such as activity across many channels or neurons) into a smaller number of variables, used both within spike sorting algorithms and in analyses of population activity.

Dipole
A simplified model of a neural current source in which current flows between two spatially separated poles, producing an extracellular electric field whose voltage falls off with distance from the source.

Ground truth
Data in which the true spike times and identities of neurons are independently verified (for example, via simultaneous extracellular and intracellular recording), used as a benchmark to evaluate the accuracy of spike sorting algorithms.

International Brain Laboratory
(IBL). A consortium of neuroscience laboratories that uses standardized protocols across multiple sites to collect large-scale electrophysiology datasets spanning the mouse brain.

Manifold
A low-dimensional geometric structure embedded within the high-dimensional space of neural population activity, whose discovery can require simultaneous recordings from large numbers of neurons.

Microwire
A thin, insulated metal wire (typically less than 100 µm in diameter) used as an implanted neural electrode, often arranged in bundles to record extracellular activity from populations of neurons.

Optotagging
A technique in which light-sensitive opsins are expressed in a genetically defined neuronal population, such that these neurons can be identified in extracellular recordings on the basis of their low-latency spikes when illuminated.

Recording sites
The individual electrode contacts on a probe that sense the extracellular potential; their size affects the trade-off between spatial averaging of the signal and thermal noise from impedance.

Shanks
Thin, elongated structural elements of a multielectrode probe that penetrate neural tissue and carry an array of recording sites along their lengths.

Spike sorting
A computational procedure that detects extracellular voltage deflections caused by action potentials and assigns them to putative individual neural sources (units) on the basis of the consistency of their spatiotemporal waveform profiles across channels.

Spike trains
Discrete sequences of action potential times attributed to individual neurons, forming the primary data representation used in analyses of neural coding, decoding and reproducibility across laboratories.

Spike waveform
The characteristic spatiotemporal pattern of extracellular voltage deflections produced by a neuron's action potential, which can vary with cell morphology and transcriptomic type.

and algorithms suitable for using this spatial information to account for motion of the probe relative to the neurons[103,105], and the use of ultra-high-density sites therefore comprises a promising pathway towards enabling improved tracking in the future[55].

Outlook

The past decade has seen a tremendous leap forward in the tools and methods available for high-quality, robust and accessible electrophysiology, including both industrially scaled devices and an accompanying suite of open software tools and protocols. These developments have rapidly reshaped the field, enabling researchers to investigate spiking activity across distributed, multiregional circuits in a routine way. Electrophysiology already offers a perspective uniquely aligned with the brain's natural spatial and temporal scales, and continued innovations promise to make this view substantially richer over time. With luck, our current definition of 'large scale' will seem antiquated in the not-too-distant future.

Data availability

The data used to generate the images in Fig. 5 are available at public, open repositories: https://doi.org/10.6084/m9.figshare.9598406 (Steinmetz et al.[12]), https://doi.org/10.48324/dandi.000021/0.251116.2246 and https://doi.org/10.48324/dandi.000022/0.251116.2247 (Siegle et al.[15]), https://doi.org/10.6084/m9.figshare.21365598 (Ottenheimer et al.[309]), https://doi.org/10.48324/dandi.000363/0.231012.2129 (Chen et al.[13]), https://doi.org/10.48324/dandi.001260/0.250911.0744 (Le Merre et al.[18]), https://doi.org/10.48324/dandi.001326/0.250528.1957 (Kauvar et al.[310]), https://doi.org/10.6084/m9.figshare.19493588 (Ye et al.[55]), https://www.internationalbrainlab.com/brainwide-map (International Brain Laboratory (IBL)[19]) and https://doi.org/10.48324/dandi.000713/0.240702.1725 (Bennett et al.[311]).

Published online: 1 May 2026

References

1. Herculano-Houzel, S., Catania, K., Manger, P. R. & Kaas, J. H. Mammalian brains are made of these: a dataset of the numbers and densities of neuronal and nonneuronal cells in the brain of glires, primates, scandentia, eulipotyphlans, afrotherians and artiodactyls, and their relationship with body mass. *Brain. Behav. Evol.* **86**, 145–163 (2015).
2. Kaszás, A. et al. Capturing the electrical activity of all cortical neurons: are solutions within reach? *Adv. Sci.* **12**, e06225 (2025).
   This article evaluates whether current neural interface technologies can realistically scale to record the activity of every cortical neuron, highlighting fundamental physical and biological constraints.
3. Wilson, M. & McNaughton, B. L. Reactivation of hippocampal ensemble memories during sleep. *Science* **265**, 5–8 (1994).
4. Amaral, D. G., Ishizuka, N. & Claiborne, B. Neurons, numbers and the hippocampal network. *Prog. Brain Res.* **83**, 1–11 (1990).
5. Baeg, E. H. et al. Dynamics of population code for working memory in the prefrontal cortex. *Neuron* **40**, 177–188 (2003).
6. Quian Quiroga, R., Reddy, L., Koch, C. & Fried, I. Decoding visual inputs from multiple neurons in the human temporal lobe. *J. Neurophysiol.* **98**, 1997–2007 (2007).
7. Miura, K., Mainen, Z. F. & Uchida, N. Odor representations in olfactory cortex: distributed rate coding and decorrelated population activity. *Neuron* **74**, 1087–1098 (2012).
8. Willett, F. R. et al. A high-performance speech neuroprosthesis. *Nature* **620**, 1031–1036 (2023).
9. Steinmetz, N. A., Koch, C., Harris, K. D. & Carandini, M. Challenges and opportunities for large-scale electrophysiology with Neuropixels probes. *Curr. Opin. Neurobiol.* **50**, 92–100 (2018).
10. Gardner, R. J. et al. Toroidal topology of population activity in grid cells. *Nature* **602**, 123–128 (2022).
    By recording hundreds of grid cells simultaneously, this study uncovers low-dimensional population dynamics that would be invisible in smaller samples.
11. Allen, W. E. et al. Thirst regulates motivated behavior through modulation of brainwide neural population dynamics. *Science* **3932**, eaav3932 (2019).
12. Steinmetz, N. A., Zatka-Haas, P., Carandini, M. & Harris, K. D. Distributed coding of choice, action and engagement across the mouse brain. *Nature* **576**, 266–273 (2019).

13. Chen, S. et al. Brain-wide neural activity underlying memory-guided movement. *Cell* **187**, 676–691.e16 (2024).
This paper exemplifies the scale of data that can now be collected in a single study, revealing a close relationship between neural dynamics and anatomical organization.
14. Khilkevich, A. et al. Brain-wide dynamics linking sensation to action during decision-making. *Nature* **634**, 890–900 (2024).
15. Siegle, J. et al. Survey of spiking in the mouse visual system reveals functional hierarchy. *Nature* **592**, 86–92 (2021).
16. Strickland, J. A. & McDannald, M. A. Brainstem networks construct threat probability and prediction error from neuronal building blocks. *Nat. Commun.* **13**, 6192 (2022).
17. Stagkourakis, S. et al. Anatomically distributed neural representations of instincts in the hypothalamus. Preprint at *bioRxiv* https://doi.org/10.1101/2023.11.21.568163 (2023).
18. Le Merre, P. et al. A prefrontal cortex map based on single neuron activity. *Nat. Neurosci.* **29**, 673–681 (2026).
19. International Brain Laboratory et al. A brain-wide map of neural activity during complex behaviour. *Nature* **645**, 177–191 (2025).
In this work, a consortium of laboratories collaboratively undertakes the collection and analysis of an electrophysiological dataset at single-neuron resolution covering approximately 300 brain regions, obtained from mice performing a cognitively demanding visual decision task.
20. Pessoa, L. The entangled brain. *J. Cogn. Neurosci.* **35**, 349–360 (2023).
21. Rosen, M. C. & Freedman, D. J. How distributed is the brain-wide network that is recruited for cognition? *Nat. Rev. Neurosci.* **27**, 138–150 (2026).
22. Hayden, B. Y., Heilbronner, S. R. & Yoo, S. B. M. Rethinking the centrality of brain areas in understanding functional organization. *Nat. Neurosci.* **29**, 267–278 (2026).
23. Murray, J. D. et al. A hierarchy of intrinsic timescales across primate cortex. *Nat. Neurosci.* **17**, 1661–1663 (2014).
24. Shi, Y.-L., Zeraati, R., Levina, A. & Engel, T. A. Brain-wide organization of intrinsic timescales at single-neuron resolution. Preprint at *bioRxiv* https://doi.org/10.1101/2025.08.30.673281 (2025).
25. Song, M. et al. Hierarchical gradients of multiple timescales in the mammalian forebrain. *Proc. Natl. Acad. Sci. USA* **121**, e2415695121 (2024).
26. Okun, M., Steinmetz, N. A., Lak, A., Dervinis, M. & Harris, K. D. Distinct structure of cortical population activity on fast and infraslow timescales. *Cereb. Cortex* **29**, 2196–2210 (2019).
27. Buzsaki, G. *Rhythms of the Brain* (Oxford Univ. Press, 2006).
28. Joo, H. R. & Frank, L. M. The hippocampal sharp wave–ripple in memory retrieval for immediate use and consolidation. *Nat. Rev. Neurosci.* **19**, 744–757 (2018).
29. Bimbard, C., Harris, K. D. & Carandini, M. Invariant activity sequences across the mouse brain. Preprint at *bioRxiv* https://doi.org/10.64898/2025.12.20.695676 (2026).
30. Fischer, B. & Boch, R. Saccadic eye movements after extremely short reaction times in the monkey. *Brain Res.* **260**, 21–26 (1983).
31. Burgess, C. P. et al. High-yield methods for accurate two-alternative visual psychophysics in head-fixed mice. *Cell Rep.* **20**, 2513–2524 (2017).
32. Buzsáki, G., Anastassiou, C. A. & Koch, C. The origin of extracellular fields and currents—EEG, ECoG, LFP and spikes. *Nat. Rev. Neurosci.* **13**, 407–420 (2012).
33. Halnes, G. et al. *Electric Brain Signals: Foundations and Applications of Biophysical Modeling* (Cambridge Univ. Press, 2024).
This work presents a comprehensive treatment of the physics and biophysical modelling frameworks needed to link neuronal activity to extracellular recordings across spatial scales.
34. Adrian, E. D. The impulses produced by sensory nerve endings: part I. *J. Physiol.* **61**, 49–72 (1926).
35. Renshaw, B., Forbes, A. & Morison, B. R. Activity of isocortex and hippocampus: electrical studies with micro-electrodes. *J. Neurophysiol.* **3**, 74–105 (1940).
36. Marblestone, A. H. et al. Physical principles for scalable neural recording. *Front. Comput. Neurosci.* **7**, 137 (2013).
37. Kleinfeld, D. et al. Can one concurrently record electrical spikes from every neuron in a mammalian brain? *Neuron* **103**, 1005–1015 (2019).
38. Buzsáki, G. Large-scale recording of neural ensembles. *Nat. Neurosci.* **5**, 446–451 (2004).
This early perspective on large-scale electrophysiology articulates the need for simultaneous recordings across neural populations and anticipates many of the technological and analytical challenges that have since driven the field's development.
39. Henze, D. A. et al. Intracellular features predicted by extracellular recordings in the hippocampus in vivo. *J. Neurophysiol.* **84**, 390–400 (2000).
40. Fiáth, R. et al. Slow insertion of silicon probes improves the quality of acute neuronal recordings. *Sci. Rep.* **9**, 111 (2019).
41. Roitbak, A. I. & Bobrov, A. V. Spreading depression resulting from cortical punctures. *Acta Neurobiol. Exp.* **35**, 761–768 (1975).
42. Szarowski, D. H. et al. Brain responses to micro-machined silicon devices. *Brain Res.* **983**, 23–35 (2003).
43. Otte, E., Vlachos, A. & Asplund, M. Engineering strategies towards overcoming bleeding and glial scar formation around neural probes. *Cell Tissue Res.* **387**, 461–477 (2022).
44. Gold, C., Henze, D. A., Koch, C. & Buzsáki, G. On the origin of the extracellular action potential waveform: a modeling study. *J. Neurophysiol.* **95**, 3113–3128 (2006).
45. Cooper, G. F., Robson, J. G. & Waldron, I. The action potentials recorded from undamaged nerve fibres with micro-electrodes. *J. Physiol.* **200**, 9P–11P (1969).
46. Merrill, E. G., Wall, P. D. & Yaksh, T. L. Properties of two unmyelinated fibre tracts of the central nervous system: lateral Lissauer tract, and parallel fibres of the cerebellum. *J. Physiol.* **284**, 127–145 (1978).
47. Goldberg, J. H. & Fee, M. S. A cortical motor nucleus drives the basal ganglia-recipient thalamus in singing birds. *Nat. Neurosci.* **15**, 620–627 (2012).
48. Robbins, A., Fox, S., Holmes, G., Scott, R. & Barry, J. Short duration waveforms recorded extracellularly from freely moving rats are representative of axonal activity. *Front. Neural Circuits* **7**, 181 (2013).
49. Deligkaris, K., Bullmann, T. & Frey, U. Extracellularly recorded somatic and neuritic signal shapes and classification algorithms for high-density microelectrode array electrophysiology. *Front. Neurosci.* **10**, 421 (2016).
50. Schröder, S. et al. Arousal modulates retinal output. *Neuron* **107**, 487–495.e9 (2020).
51. Barthó, P. Extracellular recording of axonal spikes in the visual cortex. *J. Physiol.* **599**, 2131–2131 (2021).
52. Sun, S. H. et al. Analysis of extracellular spike waveforms and associated receptive fields of neurons in cat primary visual cortex. *J. Physiol.* **599**, 2211–2238 (2021).
53. Someck, S. et al. Positive and biphasic extracellular waveforms correspond to return currents and axonal spikes. *Commun. Biol.* **6**, 950 (2023).
54. Jia, X. et al. High-density extracellular probes reveal dendritic backpropagation and facilitate neuron classification. *J. Neurophysiol.* **121**, 1831–1847 (2019).
55. Ye, Z. et al. Ultra-high-density Neuropixels probes improve detection and identification in neuronal recordings. *Neuron* **113**, 3966–3982.e12 (2025).
This work introduces a version of the Neuropixels 1.0 probe with 10× higher site density, providing unparalleled resolution of extracellular potentials, and revealing distinctions between the spatiotemporal waveforms of different neuron types and compartments.
56. Sibille, J. et al. High-density electrode recordings reveal strong and specific connections between retinal ganglion cells and midbrain neurons. *Nat. Commun.* **13**, 5218 (2022).
57. Sibille, J., Gehr, C. & Kremkow, J. Efficient mapping of the thalamocortical monosynaptic connectivity in vivo by tangential insertions of high-density electrodes in the cortex. *Proc. Natl. Acad. Sci. USA* **121**, e2313048121 (2024).
This work uses the sensitivity and scale of Neuropixels recordings to capture both thalamocortical axons and their cortical postsynaptic targets, enabling the study of synaptic plasticity in vivo.
58. Berke, J. D., Okatan, M., Skurski, J. & Eichenbaum, H. B. Oscillatory entrainment of striatal neurons in freely moving rats. *Neuron* **43**, 883–896 (2004).
59. Canakci, S., Toy, M. F., Inci, A. F., Liu, X. & Kuzum, D. Computational analysis of network activity and spatial reach of sharp wave-ripples. *PLoS One* **12**, e0184542 (2017).
60. Viswam, V., Obien, M., Frey, U., Franke, F. & Hierlemann, A. Acquisition of bioelectrical signals with small electrodes. *IEEE Biomed. Circuits Syst. Conf.* **2017**, 1–4 (2017).
61. Hill, M. et al. Quantitative simulation of extracellular single unit recording from the surface of cortex. *J. Neural Eng.* **15**, 056007 (2018).
62. Luan, L., Yin, R., Zhu, H. & Xie, C. Emerging penetrating neural electrodes: in pursuit of large scale and longevity. *Annu. Rev. Biomed. Eng.* **25**, 185–205 (2023).
63. Cui, X. & Martin, D. C. Electrochemical deposition and characterization of poly(3,4-ethylenedioxythiophene) on neural microelectrode arrays. *Sens. Actuators B Chem.* **89**, 92–102 (2003).
64. Ludwig, K. A. et al. Poly(3,4-ethylenedioxythiophene) (PEDOT) polymer coatings facilitate smaller neural recording electrodes. *J. Neural Eng.* **8**, 014001 (2011).
65. Mora Lopez, C. et al. A neural probe with up to 966 electrodes and up to 384 configurable channels in 0.13 µm SOI CMOS. *IEEE Trans. Biomed. Circuits Syst.* **11**, 510–522 (2017).
66. Kozai, T. D. Y. & Vazquez, A. L. Photoelectric artefact from optogenetics and imaging on microelectrodes and bioelectronics: new challenges and opportunities. *J. Mater. Chem. B* **3**, 4965–4978 (2015).
67. Stringer, C. et al. Spontaneous behaviors drive multidimensional, brainwide activity. *Science* **364**, 255 (2019).
68. Kauvar, I. V. et al. Cortical observation by synchronous multifocal optical sampling reveals widespread population encoding of actions. *Neuron* **107**, 351–367.e19 (2020).
69. Manley, J. et al. Simultaneous, cortex-wide dynamics of up to 1 million neurons reveal unbounded scaling of dimensionality with neuron number. *Neuron* **112**, 1694–1709.e5 (2024).
70. Zhang, Y. et al. Fast and sensitive GCaMP calcium indicators for imaging neural populations. *Nature* **615**, 884–891 (2023).
71. Huang, L. et al. Relationship between simultaneously recorded spiking activity and fluorescence signal in GCaMP6 transgenic mice. *eLife* **10**, e51675 (2021).
72. Berens, P. et al. Community-based benchmarking improves spike rate inference from two-photon calcium imaging data. *PLOS Comput. Biol.* **14**, e1006157 (2018).
73. Friedrich, J., Zhou, P. & Paninski, L. Fast online deconvolution of calcium imaging data. *PLOS Comput. Biol.* **13**, e1005423 (2017).
74. Pachitariu, M., Stringer, C. & Harris, K. D. Robustness of spike deconvolution for neuronal calcium imaging. *J. Neurosci.* **38**, 7976–7985 (2018).
75. Rupprecht, P., Rózsa, M., Fang, X., Svoboda, K. & Helmchen, F. Spike inference from calcium imaging data acquired with GCaMP8 indicators. Preprint at *bioRxiv* https://doi.org/10.1101/2025.03.03.641129 (2025).
76. Theis, L. et al. Benchmarking spike rate inference in population calcium imaging. *Neuron* **90**, 471–482 (2016).
77. Bai, L. et al. Volumetric voltage imaging of neuronal populations in the mouse brain by confocal light-field microscopy. *Nat. Methods* **21**, 2160–2170 (2024).
78. Prevedel, R. et al. Three-photon microscopy: an emerging technique for deep intravital brain imaging. *Nat. Rev. Neurosci.* **26**, 521–537 (2025).
79. Barretto, R. P. & Schnitzer, M. J. In vivo microendoscopy of the hippocampus. *Cold Spring Harb. Protoc.* **2012**, 1092–1099 (2012).

80. Xiao, S. et al. Large-scale deep tissue voltage imaging with targeted-illumination confocal microscopy. *Nat. Methods* **21**, 1094–1102 (2024).
81. Sofroniew, N. J., Flickinger, D., King, J. & Svoboda, K. A large field of view two-photon mesoscope with subcellular resolution for in vivo imaging. *eLife* **5**, e14472 (2016).
82. Clough, M. et al. Flexible simultaneous mesoscale two-photon imaging of neural activity at high speeds. *Nat. Commun.* **12**, 6638 (2021).
83. Yu, C.-H., Stirman, J. N., Yu, Y., Hira, R. & Smith, S. L. Diesel2p mesoscope with dual independent scan engines for flexible capture of dynamics in distributed neural circuitry. *Nat. Commun.* **12**, 6639 (2021).
84. McCormick, D. A., Connors, B. W., Lighthall, J. W. & Prince, D. A. Comparative electrophysiology of pyramidal and sparsely spiny stellate neurons of the neocortex. *J. Neurophysiol.* **54**, 782–806 (1985).
85. Barthó, P. et al. Characterization of neocortical principal cells and interneurons by network interactions and extracellular features. *J. Neurophysiol.* **92**, 600–608 (2004).
86. Mitchell, J. F., Sundberg, K. A. A. & Reynolds, J. H. Differential attention-dependent response modulation across cell classes in macaque visual area V4. *Neuron* **55**, 131–141 (2007).
87. Niell, C. M. & Stryker, M. P. Highly selective receptive fields in mouse visual cortex. *J. Neurosci.* **28**, 7520–7520 (2008).
88. Yamin, H. G., Stern, E. A. & Cohen, D. Parallel processing of environmental recognition and locomotion in the mouse striatum. *J. Neurosci.* **33**, 473–484 (2013).
89. Senzai, Y. & Buzsáki, G. Physiological properties and behavioral correlates of hippocampal granule cells and mossy cells. *Neuron* **93**, 691–704.e5 (2017).
90. Yu, J., Hu, H., Agmon, A. & Svoboda, K. Recruitment of GABAergic interneurons in the barrel cortex during active tactile behavior. *Neuron* **104**, 412–427.e4 (2019).
91. Lee, E. K. et al. Non-linear dimensionality reduction on extracellular waveforms reveals cell type diversity in premotor cortex. *eLife* **10**, e67490 (2021).
92. Beau, M. et al. A deep learning strategy to identify cell types across species from high-density extracellular recordings. *Cell* **188**, 2218–2234.e22 (2025).
This work showcases the promise of cell type identification in electrophysiology by introducing a novel approach for classifying cerebellar cells on the basis of their waveforms and spiking patterns.
93. Steinmetz, N. A. et al. Aberrant cortical activity in multiple GCaMP6-expressing transgenic mouse lines. *eNeuro* https://doi.org/10.1523/ENEURO.0207-17.2017 (2017).
94. Lewis, C. M., Hoffmann, A. & Helmchen, F. Linking brain activity across scales with simultaneous opto- and electrophysiology. *Neurophotonics* **11**, 033403 (2023).
95. Ramezani, M., Ren, Y., Cubukcu, E. & Kuzum, D. Innovating beyond electrophysiology through multimodal neural interfaces. *Nat. Rev. Electr. Eng.* **2**, 42–57 (2025).
96. Clancy, K. B., Orsolic, I. & Mrsic-Flogel, T. D. Locomotion-dependent remapping of distributed cortical networks. *Nat. Neurosci.* **22**, 778–786 (2019).
97. Xiao, D. et al. Mapping cortical mesoscopic networks of single spiking cortical or sub-cortical neurons. *eLife* **6**, e19976 (2017).
98. Peters, A. J., Fabre, J. M. J., Steinmetz, N. A., Harris, K. D. & Carandini, M. Striatal activity topographically reflects cortical activity. *Nature* **591**, 420–425 (2021).
99. Yan, Y. & Murphy, T. H. Decoding state-dependent cortical-cerebellar cellular functional connectivity in the mouse brain. *Cell Rep.* **43**, 114348 (2024).
This work combines 'widefield' calcium imaging across the cortex with Neuropixels recordings in the cerebellum, revealing a surprising state dependence of these correlations between individual cerebellar neurons and cortical activity.
100. Ye, Z. et al. Brain-wide topographic coordination of traveling spiral waves. Preprint at *bioRxiv* https://doi.org/10.1101/2023.12.07.570517 (2025).
101. Li, A. J. et al. Global and local origins of trial-to-trial spike count variability in visual cortex. Preprint at *bioRxiv* https://doi.org/10.1101/2025.08.08.669442 (2025).
102. Dhawale, A. K. et al. Automated long-term recording and analysis of neural activity in behaving animals. *eLife* **6**, e27702 (2017).
103. Steinmetz, N. A. et al. Neuropixels 2.0: a miniaturized high-density probe for stable, long-term brain recordings. *Science* **372**, eabf4588 (2021).
This paper presents a multi-shank Neuropixels probe with a smaller form factor than its predecessor, along with analysis tools for stable long-term recordings from thousands of neurons.
104. Morrell, R. M. Control of cortical pulsations. *Electroencephalogr. Clin. Neurophysiol.* **10**, 739–740 (1958).
105. Windolf, C. et al. DREDge: robust motion correction for high-density extracellular recordings across species. *Nat. Methods* **22**, 788–800 (2025).
This paper introduces a novel, state-of-the-art algorithm for correcting for motion of the brain relative to recording electrodes, a critical ongoing challenge in large-scale electrophysiology data analysis.
106. Nurmikko, A. Challenges for large-scale cortical interfaces. *Neuron* **108**, 259–269 (2020).
107. Nordhausen, C. T., Rousche, P. J. & Normann, R. A. Optimizing recording capabilities of the Utah Intracortical Electrode Array. *Brain Res.* **637**, 27–36 (1994).
108. Maynard, E. M., Nordhausen, C. T. & Normann, R. A. The Utah Intracortical Electrode Array: a recording structure for potential brain–computer interfaces. *Electroencephalogr. Clin. Neurophysiol.* **102**, 228–239 (1997).
109. Sahasrabuddhe, K. et al. The Argo: a high channel count recording system for neural recording in vivo. *J. Neural Eng.* **18**, 015002 (2021).
110. Chen, X. et al. Chronic stability of a neuroprosthesis comprising multiple adjacent Utah arrays in monkeys. *J. Neural Eng.* **20**, 036039 (2023).
111. Papale, P., Wang, F., Self, M. W. & Roelfsema, P. R. An extensive dataset of spiking activity to reveal the syntax of the ventral stream. *Neuron* **113**, 539–553.e5 (2025).
112. Wise, K. D., Angell, J. B. & Starr, A. An integrated-circuit approach to extracellular microelectrodes. *IEEE Trans. Biomed. Eng.* **17**, 238–247 (1970).
113. Seymour, J. P. & Kipke, D. R. Neural probe design for reduced tissue encapsulation in CNS. *Biomaterials* **28**, 3594–3607 (2007).
114. Stice, P., Gilletti, A., Panitch, A. & Muthuswamy, J. Thin microelectrodes reduce GFAP expression in the implant site in rodent somatosensory cortex. *J. Neural Eng.* **4**, 42 (2007).
115. Karumbaiah, L. et al. Relationship between intracortical electrode design and chronic recording function. *Biomaterials* **34**, 8061–8074 (2013).
116. Scholvin, J. et al. Close-packed silicon microelectrodes for scalable spatially oversampled neural recording. *IEEE Trans. Biomed. Eng.* **63**, 120–130 (2016).
117. Shobe, J. L., Claar, L. D., Parhami, S., Bakhurin, K. I. & Masmanidis, S. C. Brain activity mapping at multiple scales with silicon microprobes containing 1,024 electrodes. *J. Neurophysiol.* **114**, 2043–2052 (2015).
118. Rios, G., Lubenov, E. V., Chi, D., Roukes, M. L. & Siapas, A. G. Nanofabricated neural probes for dense 3D recordings of brain activity. *Nano Lett.* **16**, 6857–6862 (2016).
119. Jun, J. J. et al. Fully integrated silicon probes for high-density recording of neural activity. *Nature* **551**, 232–236 (2017).
This paper introduces the Neuropixels probe, which has since become the dominant technology for large-scale extracellular electrophysiology.
120. Bennett, C. et al. SHIELD: skull-shaped hemispheric implants enabling large-scale electrophysiology datasets in the mouse brain. *Neuron* **112**, 2869–2885.e8 (2024).
121. Vesuna, S. et al. Deep posteromedial cortical rhythm in dissociation. *Nature* **586**, 87–94 (2020).
122. MacDowell, C. J., Libby, A., Jahn, C. I., Tafazoli, S. & Buschman, T. J. Multiplexed subspaces route neural activity across brain-wide networks. *Nat. Commun.* **16**, 3359 (2025).
123. Luo, T. Z. et al. An approach for long-term, multi-probe Neuropixels recordings in unrestrained rats. *eLife* **9**, e59716 (2020).
124. Bondy, A. G. et al. Brain-wide coordination of decision formation and commitment. Preprint at *bioRxiv* https://doi.org/10.1101/2024.08.21.609044 (2025).
This work implants eight Neuropixels 1.0 probes in rats, yielding >3,000 simultaneously sampled channels, permitting a view at single-neuron resolution across a broad network of interconnected brain regions while rats performed a sophisticated decision-making task.
125. Khanna, A. R. et al. Single-neuronal elements of speech production in humans. *Nature* **626**, 603–610 (2024).
126. Leonard, M. K. et al. Large-scale single-neuron speech sound encoding across the depth of human cortex. *Nature* **626**, 593–602 (2024).
127. Bigelow, A., Kim, T., Namima, T., Bair, W. & Pasupathy, A. Dissociation in neuronal encoding of object versus surface motion in the primate brain. *Curr. Biol.* **33**, 711–719.e5 (2023).
128. Namima, T. et al. Inserting a Neuropixels probe into awake monkey cortex: two probes, two methods. *J. Neurosci. Methods* **402**, 110016 (2024).
129. Trautmann, E. M. et al. Accurate estimation of neural population dynamics without spike sorting. *Neuron* **103**, 292–308 (2019).
130. Zhang, L. A., Li, P. & Callaway, E. M. High-resolution laminar identification in macaque primary visual cortex using Neuropixels probes. Preprint at *bioRxiv* https://doi.org/10.1101/2024.01.23.576944 (2024).
131. Zhu, S., Oh, Y. J., Trepka, E. B., Chen, X. & Moore, T. Dependence of contextual modulation in macaque V1 on interlaminar signal flow. *eLife* **13**, RP103255 (2026).
132. Dotson, N. M., Davis, Z. W., Jendritza, P. & Reynolds, J. H. Acute Neuropixels recordings in the marmoset monkey. *eNeuro* **11**, ENEURO.0544-23.2024 (2024).
133. Lanfranchi, F. F., Wekselblatt, J., Wagenaar, D. A. & Tsao, D. Y. A compressed hierarchy for visual form processing in the tree shrew. *Nature* **646**, 872–882 (2025).
134. Town, S. M., Poole, K. C., Wood, K. C. & Bizley, J. K. Reversible inactivation of ferret auditory cortex impairs spatial and nonspatial hearing. *J. Neurosci.* **43**, 749–763 (2023).
135. Forli, A., Fan, W., Qi, K. K. & Yartsev, M. M. Replay and representation dynamics in the hippocampus of freely flying bats. *Nature* **645**, 974–980 (2025).
136. Fenk, L. A., Riquelme, J. L. & Laurent, G. Interhemispheric competition during sleep. *Nature* **616**, 312–318 (2023).
137. Haggard, M. & Chacron, M. J. Coding of object location by heterogeneous neural populations with spatially dependent correlations in weakly electric fish. *PLoS Comput. Biol.* **19**, e1010938 (2023).
138. Metzen, M. G. & Chacron, M. J. Population coding of natural electrosensory stimuli by midbrain neurons. *J. Neurosci.* **41**, 3822–3841 (2021).
139. Pedraja, F. et al. Direct cerebellar control over motor production in a species with extreme cerebellar enlargement. *Curr. Biol.* **35**, 3515–3522.e4 (2025).
140. Torok, Z. et al. Resilience of a learned motor behavior after chronic disruption of inhibitory circuits. *eLife* **14**, RP106039 (2025).
141. Tostado-Marcos, P. et al. Population dynamics in songbird RA and HVC during learned motor-vocal behavior. *J. Neurosci.* https://doi.org/10.1523/JNEUROSCI.0580-25.2026 (2026).
142. Pophale, A. et al. Wake-like skin patterning and neural activity during octopus sleep. *Nature* **619**, 129–134 (2023).
This work records neural activity from the octopus brain with Neuropixels 1.0 probes, highlighting the broad applicability of electrophysiological tool development across the animal kingdom.

143. Alcalá, R. J. I. et al. A modular, adaptable, and accessible implant kit for chronic electrophysiological recordings in rats. *Cell Rep. Methods* **5**, 101146 (2025).
144. Balogh-Lantos, Z., Fiáth, R., Horváth, ÁC. & Fekete, Z. High density laminar recordings reveal cell type and layer specific responses to infrared neural stimulation in the rat neocortex. *Sci. Rep.* **14**, 31523 (2024).
145. Cheng, A. et al. SCREWx: a screwless, chronic, recoverable, and lightweight Neuropixels fixture for freely-moving rodents. Preprint at *bioRxiv* https://doi.org/10.64898/2026.01.06.697790 (2026).
146. Concha-Miranda, M., Tang, W., Hartmann, K. & Brecht, M. Large-scale mapping of vocalization-related activity in the functionally diverse nuclei in rat posterior brainstem. *J. Neurosci.* **42**, 8252–8261 (2022).
147. Demetrovich, P. G. & Colgin, L. L. Dynamics of dentate gyrus place cells and dentate spikes signal spatial and nonspatial changes in environments. Preprint at *bioRxiv* https://doi.org/10.1101/2025.10.24.684382 (2025).
148. Findlay, G. et al. A hippocampal 'sharp-wave sleep' state that is dissociable from cortical sleep. *Nat. Neurosci.* **29**, 399–410 (2026).
149. Ghestem, A. et al. Long-term near-continuous recording with Neuropixels probes in healthy and epileptic rats. *J. Neural Eng.* **20**, 046003 (2023).
150. Horan, M. et al. Repix: reliable, reusable, versatile chronic Neuropixels implants using minimal components. *eLife* **13**, RP98977 (2024).
This work presents a chronic implant fixture that enables recovery and reuse of Neuropixels probes after data collection, with an emphasis on low weight, stability of recordings and ease of implementation.
151. Song, Z. et al. Chronic, reusable, multiday Neuropixels recordings during free-moving operant behavior. *eNeuro* **11**, ENEURO.0245-23.2023 (2024).
152. van Daal, R. J. J. et al. Implantation of Neuropixels probes for chronic recording of neuronal activity in freely behaving mice and rats. *Nat. Protoc.* **16**, 3322–3347 (2021).
153. Yuan, L. et al. Time cell sequences during delay intervals are not dependent on brain state and do not support hippocampus-dependent working memory. *Nat. Commun.* **16**, 7470 (2025).
154. Melin, M. D., Churchland, A. K. & Couto, J. Large scale, simultaneous chronic neural recordings from multiple brain areas. Preprint at *bioRxiv* https://doi.org/10.1101/2023.12.22.572441 (2024).
155. Trautmann, E. M. et al. Large-scale high-density brain-wide neural recording in nonhuman primates. *Nat. Neurosci.* **28**, 1562–1575 (2025).
156. Orban, G. et al. Simultaneous high-density 512-channel SiNAPS electrical recordings and optogenetics. *Ann. Int. Conf. IEEE Eng. Med. Biol. Soc.* **2024**, 1–4 (2024).
157. Angotzi, G. N. et al. SiNAPS: an implantable active pixel sensor CMOS-probe for simultaneous large-scale neural recordings. *Biosens. Bioelectron.* **126**, 355–364 (2019).
This paper describes a probe architecture that integrates amplification beneath each electrode, enabling simultaneous recording from hundreds of sites.
158. Angotzi, G. N. et al. Multi-shank 1024 channels active SiNAPS probe for large multi-regional topographical electrophysiological mapping of neural dynamics. *Adv. Sci.* **12**, 2416239 (2025).
159. Khanzada, S. et al. Experience reorganizes coordinated population dynamics across hippocampal circuits. Preprint at *bioRxiv* https://doi.org/10.64898/2026.01.15.698118 (2026).
160. Gonzalez, J. et al. Subspace communication in the hippocampal–retrosplenial axis. Preprint at *bioRxiv* https://doi.org/10.64898/2025.12.31.697203 (2026).
161. Paleologos, N. et al. Electroanatomy of hippocampal activity patterns: theta, gamma waves, sharp wave-ripples, and dentate spikes. *Front. Behav. Neurosci.* **19**, 1685846 (2025).
162. Maslarova, A. et al. Spatiotemporal patterns differentiate hippocampal sharp-wave ripples from interictal epileptiform discharges in mice and humans. *Nat. Commun.* **16**, 11636 (2025).
163. Angotzi, G. N. et al. High-density, identified cell recordings from motor cortex of awake behaving macaques using 1024-channel SiNAPS-NHP probes. Preprint at *bioRxiv* https://doi.org/10.1101/2025.07.22.665434 (2025).
164. Hong, G. & Lieber, C. M. Novel electrode technologies for neural recordings. *Nat. Rev. Neurosci.* **20**, 330–345 (2019).
165. Orlemann, C. et al. Friend, not foe: lowered tissue reactivity to long-term polyimide implants. Preprint at *bioRxiv* https://doi.org/10.64898/2026.02.06.703281 (2026).
166. Woods, D. P. et al. Repeatable, low-drift recordings in behaving non-human primates using flexible microelectrodes. Preprint at *bioRxiv* https://doi.org/10.64898/2026.01.09.698500 (2026).
167. Chung, J. E. et al. High-density, long-lasting, and multi-region electrophysiological recordings using polymer electrode arrays. *Neuron* **101**, 21–31.e5 (2019).
168. Zhao, Z. et al. Ultraflexible electrode arrays for months-long high-density electrophysiological mapping of thousands of neurons in rodents. *Nat. Biomed. Eng.* **7**, 520–532 (2023).
This paper demonstrates 1,000+ channel recordings with flexible probes, which can be used to record from the same populations of neurons over months.
169. Barz, F., Trouillet, V., Paul, O. & Ruther, P. CMOS-compatible, flexible, intracortical neural probes. *IEEE Trans. Biomed. Eng.* **67**, 1366–1376 (2020).
170. De Dorigo, D. et al. Fully immersible subcortical neural probes with modular architecture and a ΔΣ ADC integrated under each electrode for parallel readout of 144 recording sites. *IEEE J. Solid-State Circuits* **53**, 3111–3125 (2018).
171. Park, S.-Y. et al. A miniaturized 256-channel neural recording interface with area-efficient hybrid integration of flexible probes and CMOS integrated circuits. *IEEE Trans. Biomed. Eng.* **69**, 334–346 (2022).
172. Zhao, E. T. et al. A CMOS-based highly scalable flexible neural electrode interface. *Sci. Adv.* **9**, eadf9524 (2023).
173. Luan, L. et al. Recent advances in electrical neural interface engineering: minimal invasiveness, longevity, and scalability. *Neuron* **108**, 302–321 (2020).
174. Williams, N. P. et al. In vivo microelectrode arrays for neuroscience. *Nat. Rev. Methods Primer* **5**, 31 (2025).
175. Gray, C. M., Maldonado, P. E., Wilson, M. & McNaughton, B. Tetrodes markedly improve the reliability and yield of multiple single-unit isolation from multi-unit recordings in cat striate cortex. *J. Neurosci. Methods* **63**, 43–54 (1995).
176. Lubenov, E. V. & Siapas, A. G. Hippocampal theta oscillations are travelling waves. *Nature* **459**, 534–539 (2009).
177. Voigts, J., Newman, J. P., Wilson, M. A. & Harnett, M. T. An easy-to-assemble, robust, and lightweight drive implant for chronic tetrode recordings in freely moving animals. *J. Neural Eng.* **17**, 026044 (2020).
178. Widloski, J. & Foster, D. J. Flexible rerouting of hippocampal replay sequences around changing barriers in the absence of global place field remapping. *Neuron* **110**, 1547–1558.e8 (2022).
179. Campagner, D. et al. Aeon: an open-source platform to study the neural basis of ethological behaviours over naturalistic timescales. Preprint at *bioRxiv* https://doi.org/10.1101/2025.07.31.664513 (2025).
180. Juavinett, A. L., Bekheet, G. & Churchland, A. K. Chronically implanted Neuropixels probes enable high-yield recordings in freely moving mice. *eLife* **8**, e47188 (2019).
181. Newman, J. P. et al. ONIX: a unified open-source platform for multimodal neural recording and perturbation during naturalistic behavior. *Nat. Methods* **22**, 187–192 (2025).
182. Fink, A. J. P. et al. Experience-dependent reorganization of inhibitory neuron synaptic connectivity. Preprint at *bioRxiv* https://doi.org/10.1101/2025.01.16.633450 (2025).
183. Jones, E. A. A. Chronic recoverable Neuropixels in mice. *protocols.io* https://doi.org/10.17504/protocols.io.e6nvwjo87lmk/v1 (2023).
184. Bimbard, C. et al. An adaptable, reusable, and light implant for chronic Neuropixels probes. *eLife* **13**, RP98522 (2025).
185. Kozai, T. D. Y. et al. Reduction of neurovascular damage resulting from microelectrode insertion into the cerebral cortex using in vivo two-photon mapping. *J. Neural Eng.* **7**, 046011 (2010).
186. Durand, S. et al. Acute head-fixed recordings in awake mice with multiple Neuropixels probes. *Nat. Protoc.* **18**, 424–457 (2023).
187. Navabi, Z. S. et al. Computer vision guided rapid and precise automated cranial microsurgeries in rodents. Preprint at *bioRxiv* https://doi.org/10.1101/2024.09.03.611036 (2024).
188. Chung, J. E. et al. High-density single-unit human cortical recordings using the Neuropixels probe. *Neuron* **110**, 2409–2421.e3 (2022).
189. Paulk, A. C. et al. Large-scale neural recordings with single neuron resolution using Neuropixels probes in human cortex. *Nat. Neurosci.* **25**, 252–263 (2022).
Together with Chung et al. (2022), this work is one of the earliest studies to use high-density electrode arrays to record from isolated neurons across the depth of human cortex.
190. Jamali, M. et al. Semantic encoding during language comprehension at single-cell resolution. *Nature* **631**, 610–616 (2024).
191. Chung, J. E. et al. Experience and safety of intraoperative Neuropixels: a case series of 56 patients. *J. Neurosurg.* **144**, 63–73 (2025).
192. Brown, D. E. et al. High-density multi-depth human recordings using 45 mm long Neuropixels probes. Preprint at https://doi.org/10.48550/arXiv.2601.09912 (2026).
193. Coughlin, B. et al. Modified Neuropixels probes for recording human neurophysiology in the operating room. *Nat. Protoc.* **18**, 2927–2953 (2023).
194. Einevoll, G. T., Franke, F., Hagen, E., Pouzat, C. & Harris, K. D. Towards reliable spike-train recordings from thousands of neurons with multielectrodes. *Curr. Opin. Neurobiol.* **22**, 11–17 (2012).
195. Hubel, D. H. Tungsten microelectrode for recording from single units. *Science* **125**, 549–550 (1957).
196. Pachitariu, M., Steinmetz, N. A., Kadir, S. N., Carandini, M. & Harris, K. D. in *Advances in Neural Information Processing Systems* Vol. 29 (eds Lee, D. D., Sugiyama, M., Luxburg, U. V., Guyon, I. & Garnett, R.) 4448–4456 (Curran, 2016).
197. Pachitariu, M., Sridhar, S., Pennington, J. & Stringer, C. Spike sorting with Kilosort4. *Nat. Methods* **21**, 914–921 (2024).
This work presents the most widely used spike sorting algorithm for large-scale recordings on the basis of its accuracy, its minimal need for parameter tuning, and its speed and scalability.
198. Yger, P. et al. A spike sorting toolbox for up to thousands of electrodes validated with ground truth recordings in vitro and in vivo. *eLife* **7**, e34518 (2018).
199. Lee, J. et al. YASS: Yet Another Spike Sorter applied to large-scale multi-electrode array recordings in primate retina. Preprint at *bioRxiv* https://doi.org/10.1101/2020.03.18.997924 (2020).
200. Boussard, J. et al. DARTsort: a modular drift tracking spike sorter for high-density multi-electrode probes. Preprint at *bioRxiv* https://doi.org/10.1101/2023.08.11.553023 (2023).
201. Fang, T. & Zamani, M. FS-SS: few-shot learning for fast and accurate spike sorting of high-channel count probes. Preprint at https://doi.org/10.48550/arXiv.2503.18040 (2025).
202. Georgiadis, V. & Petrantonakis, P. SpikeSift: a computationally efficient and drift-resilient spike sorting algorithm. *J. Neural Eng.* https://doi.org/10.1088/1741-2552/adee48 (2025).

203. Giraud, E., Lynn, M., Vincent-Lamarre, P., Béïque, J.-C. & Thivierge, J.-P. Unsupervised pipeline for the identification of cortical excitatory and inhibitory neurons in high-density multielectrode arrays with ground-truth validation. *eLife* **14**, RP106557 (2025).
204. Lotfi, M. A., Zareayan Jahromy, F. & Daliri, M. R. Advancing spike sorting through gradient-based preprocessing and nonlinear reduction with agglomerative clustering. *Brain Behav.* **15**, e70650 (2025).
205. Muralidharan, S. et al. A system for live sorting of neuronal spiking activity from large-scale recordings. Preprint at *bioRxiv* https://doi.org/10.64898/2025.12.29.696938 (2026).
206. Buccino, A. P., Garcia, S. & Yger, P. Spike sorting: new trends and challenges of the era of high-density probes. *Prog. Biomed. Eng.* **4**, 022005 (2022).
207. Buccino, A. P. et al. SpikeInterface, a unified framework for spike sorting. *eLife* **9**, e61834 (2020).
This work presents a software package unifying preprocessing steps, spike sorting algorithms and quality metrics to enable reproducible analysis pipelines.
208. Luo, T. Z. et al. Transitions in dynamical regime and neural mode during perceptual decisions. *Nature* **646**, 1156–1166 (2025).
209. Yatsenko, D. et al. DataJoint: managing big scientific data using MATLAB or Python. Preprint at *bioRxiv* https://doi.org/10.1101/031658 (2015).
210. Cheifet, B. Promoting reproducibility with Code Ocean. *Genome Biol.* **22**, 65 (2021).
211. Abe, T. et al. Neuroscience Cloud Analysis As a Service: an open-source platform for scalable, reproducible data analysis. *Neuron* **17**, 2771–2789.e7 (2022).
212. Geng, J. et al. Multiscale cloud-based pipeline for neuronal electrophysiology analysis and visualization. Preprint at *bioRxiv* https://doi.org/10.1101/2024.11.14.623530 (2024).
213. Buccino, A. P., Sridhar, A., Feng, D., Svoboda, K. & Siegle, J. H. Efficient and reproducible pipelines for spike sorting large-scale electrophysiology data. Preprint at *bioRxiv* https://doi.org/10.1101/2025.11.12.687966 (2025).
214. Allen, B. D. et al. Automated in vivo patch-clamp evaluation of extracellular multielectrode array spike recording capability. *J. Neurophysiol.* **120**, 2182–2200 (2018).
215. Magland, J. et al. SpikeForest, reproducible web-facing ground-truth validation of automated neural spike sorters. *eLife* **9**, e55167 (2020).
216. Marques-Smith, A. et al. Recording from the same neuron with high-density CMOS probes and patch-clamp: a ground-truth dataset and an experiment in collaboration. Preprint at *bioRxiv* https://doi.org/10.1101/370080 (2020).
217. Hill, D. N., Mehta, S. B. & Kleinfeld, D. Quality metrics to accompany spike sorting of extracellular signals. *J. Neurosci.* **31**, 8699–8705 (2011).
This work highlights the need for quantitative metrics to estimate errors in spike sorter outputs, and introduces approaches that remain essential as electrophysiology scales to thousands of simultaneous channels.
218. Laquitaine, S., Imbeni, M., Tharayil, J., Isbister, J. B. & Reimann, M. W. Spike sorting biases and information loss in a detailed cortical model. Preprint at *bioRxiv* https://doi.org/10.1101/2024.12.04.626805 (2024).
219. Rossant, C. et al. Spike sorting for large, dense electrode arrays. *Nat. Neurosci.* **19**, 634 (2016).
220. Vincent, J. P. & Economo, M. N. Assessing cross-contamination in spike-sorted electrophysiology data. *eNeuro* **11**, ENEURO.0554-23.2024 (2024).
221. Gerstein, G. L. & Perkel, D. H. Simultaneously recorded trains of action potentials: analysis and functional interpretation. *Science* **164**, 828–830 (1969).
222. Zohary, E., Shadlen, M. N. & Newsome, W. T. Correlated neuronal discharge rate and its implications for psychophysical performance. *Nature* **370**, 140–143 (1994).
223. Cohen, M. R. & Kohn, A. Measuring and interpreting neuronal correlations. *Nat. Neurosci.* **14**, 811–819 (2011).
224. Roth, N. et al. A flexible quality metric for electrophysiological recordings across brain regions and species. Preprint at *bioRxiv* https://doi.org/10.64898/2026.03.06.710130 (2026).
225. Schmitzer-Torbert, N., Jackson, J., Henze, D., Harris, K. & Redish, A. D. Quantitative measures of cluster quality for use in extracellular recordings. *Neuroscience* **131**, 1–11 (2005).
226. International Brain Laboratory. Spike sorting pipeline for the International Brain Laboratory. *figshare* https://doi.org/10.6084/m9.figshare.19705522.v4 (2022).
227. FabreJ. M. J.BeestE. H.van, PetersA. J.CarandiniM.HarrisK. D. Bombcell: automated curation and cell classification of spike-sorted electrophysiology data. *Zenodo* https://doi.org/10.5281/zenodo.8172822 (2023).
228. Kloosterman, F., Layton, S. P., Chen, Z. & Wilson, M. A. Bayesian decoding using unsorted spikes in the rat hippocampus. *J. Neurophysiol.* **111**, 217–227 (2014).
229. Zhang, Y. et al. Bypassing spike sorting: density-based decoding using spike localization from dense multielectrode probes. *Adv. Neural Inf. Process. Syst.* **36**, 77604–77631 (2023).
230. Harris, K. D., Quiroga, R. Q., Freeman, J. & Smith, S. L. Improving data quality in neuronal population recordings. *Nat. Neurosci.* **19**, 1165–1174 (2016).
231. Hubel, D. H. & Wiesel, T. N. Receptive fields, binocular interaction and functional architecture in the cat's visual cortex. *J. Physiol.* **160**, 106–154 (1962).
232. O'Keefe, J. & Dostrovsky, J. The hippocampus as a spatial map. Preliminary evidence from unit activity in the freely-moving rat. *Brain Res.* **34**, 171–175 (1971).
233. International Brain Laboratory et al. Reproducibility of in vivo electrophysiological measurements in mice. *eLife* **13**, RP100840 (2025).
This work shows that recording from the same target location with the same recording apparatus in each of ten different laboratories allows for carefully assessing the reproducibility of a range of characteristics of large-scale electrophysiological recordings with Neuropixels, and the establishment of a set of recommendations for inclusion criteria.
234. Bennett, C. et al. Higher-order thalamic circuits channel parallel streams of visual information in mice. *Neuron* **102**, 477–492.e5 (2019).
235. Thomas, A. et al. Superior colliculus bidirectionally modulates choice activity in frontal cortex. *Nat. Commun.* **14**, 7358 (2023).
236. Paxinos, G. & Franklin, K. B. *Paxinos and Franklin's the Mouse Brain in Stereotaxic Coordinates* (Academic, 2019).
237. Dorr, A. E., Lerch, J. P., Spring, S., Kabani, N. & Henkelman, R. M. High resolution three-dimensional brain atlas using an average magnetic resonance image of 40 adult C57Bl/6J mice. *NeuroImage* **42**, 60–69 (2008).
238. Aggarwal, M., Zhang, J., Miller, M. I., Sidman, R. L. & Mori, S. Magnetic resonance imaging and micro-computed tomography combined atlas of developing and adult mouse brains for stereotaxic surgery. *Neuroscience* **162**, 1339–1350 (2009).
239. Kim, E., MacNicol, E., Sreedharan, J. & Cash, D. Evaluation of a new, openly accessible in vivo MP2RAGE mouse brain template for registration and morphometric analysis. *Proc. Intl Soc. Mag. Reson. Med.* **30**, 2012 (2022).
240. Perens, J. et al. Multimodal 3D mouse brain atlas framework with the skull-derived coordinate system. *Neuroinformatics* **21**, 269–286 (2023).
241. Mansour, H. et al. The Duke Mouse Brain Atlas: MRI and light sheet microscopy stereotaxic atlas of the mouse brain. *Sci. Adv.* **11**, eadq8089 (2025).
242. Birman, D. et al. Pinpoint: trajectory planning for multi-probe electrophysiology and injections in an interactive web-based 3D environment. *eLife* **12**, RP91662 (2023).
243. Liu, L. D. et al. Accurate localization of linear probe electrode arrays across multiple brains. *eNeuro* **8**, ENEURO.0241-21.202 (2021).
This work demonstrates methods for registering linear probe recordings to a common reference space, a key step for reproducible interpretation of brain-wide electrophysiology datasets.
244. Musall, S., Kaufman, M. T., Juavinett, A. L., Gluf, S. & Churchland, A. K. Single-trial neural dynamics are dominated by richly varied movements. *Nat. Neurosci.* **22**, 1677–1686 (2019).
245. Zagha, E. et al. The importance of accounting for movement when relating neuronal activity to sensory and cognitive processes. *J. Neurosci.* **42**, 1375–1382 (2022).
246. Wang, Z. A. et al. Brain-wide analysis reveals movement encoding structured across and within brain areas. *Nat. Neurosci.* **29**, 147–158 (2025).
247. Wilkinson, M. D. et al. The FAIR Guiding Principles for scientific data management and stewardship. *Sci. Data* **3**, 160018 (2016).
248. Koslow, S. H. Should the neuroscience community make a paradigm shift to sharing primary data? *Nat. Neurosci.* **3**, 863–865 (2000).
249. Martone, M. E. The past, present and future of neuroscience data sharing: a perspective on the state of practices and infrastructure for FAIR. *Front. Neuroinformatics* **17**, 1276407 (2024).
250. Teeters, J. L., Harris, K. D., Millman, K. J., Olshausen, B. A. & Sommer, F. T. Data sharing for computational neuroscience. *Neuroinformatics* **6**, 47–55 (2008).
251. Rübel, O. et al. The Neurodata Without Borders ecosystem for neurophysiological data science. *eLife* **11**, e78362 (2022).
252. Magland, J. F., Ly, R., Rübel, O. & Dichter, B. Facilitating analysis of open neurophysiology data on the DANDI Archive using large language model tools. *Sci. Data* **12**, 1988 (2025).
253. Amunts, K. et al. Linking brain structure, activity, and cognitive function through computation. *eNeuro* **9**, ENEURO.0316-21.2022 (2022).
254. Panichello, M. F. et al. Intermittent rate coding and cue-specific ensembles support working memory. *Nature* **636**, 422–429 (2024).
255. Akella, S. et al. Deciphering neuronal variability across states reveals dynamic sensory encoding. *Nat. Commun.* **16**, 1768 (2025).
256. Gao, P. & Ganguli, S. On simplicity and complexity in the brave new world of large-scale neuroscience. *Curr. Opin. Neurobiol.* **32**, 148–155 (2015).
257. Pellegrino, A., Stein, H. & Cayco-Gajic, N. A. Dimensionality reduction beyond neural subspaces with slice tensor component analysis. *Nat. Neurosci.* **27**, 1199–1210 (2024).
258. Nitzan, N., Swanson, R., Schmitz, D. & Buzsáki, G. Brain-wide interactions during hippocampal sharp wave ripples. *Proc. Natl Acad. Sci. USA* **119**, e2200931119 (2022).
259. Purandare, C. & Mehta, M. Mega-scale movie-fields in the mouse visuo-hippocampal network. *eLife* **12**, RP85069 (2023).
260. Jeong, H., Namboodiri, V. M. K., Jung, M. W. & Andermann, M. L. Sensory cortical ensembles exhibit differential coupling to ripples in distinct hippocampal subregions. *Curr. Biol.* **33**, 5185–5198.e4 (2023).
261. Farrell, J. S., Hwaun, E., Dudok, B. & Soltesz, I. Neural and behavioural state switching during hippocampal dentate spikes. *Nature* **628**, 590–595 (2024).
262. Koch, C. et al. Next-generation brain observatories. *Neuron* **110**, 3661–3666 (2022).
263. de Vries, S. E., Siegle, J. H. & Koch, C. Sharing neurophysiology data from the Allen Brain Observatory. *eLife* **12**, e85550 (2023).
264. Buccino, A. P. et al. Compression strategies for large-scale electrophysiology data. *J. Neural Eng.* **20**, 056009 (2023).
265. Lee, H. et al. Low-cost, high-efficiency double-sided neural probe. *Sens. Actuators Phys.* **387**, 116437 (2025).
266. Shin, S. et al. Novel four-sided neural probe fabricated by a thermal lamination process of polymer films. *J. Neurosci. Methods* **278**, 25–35 (2017).
267. Varga, V. et al. Working memory features are embedded in hippocampal place fields. *Cell Rep.* **43**, 113807 (2024).
268. Yang, W. et al. Selection of experience for memory by hippocampal sharp wave ripples. *Science* **383**, 1478–1483 (2024).

269. Yang, X. et al. A highly-integrated 1536-channel quad-shank monolithic neural probe in 55 nm CMOS for full-band raw-signal recording. In *2024 IEEE Symp. VLSI Technol. Circuits* 1–2 (IEEE, 2024).
270. Lee, J., Bosman, G., Green, K. R. & Ladwig, D. Noise model of gate-leakage current in ultrathin oxide MOSFETs. *IEEE Trans. Electron. Devices* **50**, 2499–2506 (2003).
271. Ribeiro, J. F. et al. ChroMOS: a "microwire-like" CMOS neural probe for chronic neural recordings in mice. *Biosens. Bioelectron.* **290**, 117942 (2025).
272. Otchy, T. M. et al. Acute off-target effects of neural circuit manipulations. *Nature* **528**, 358–363 (2015).
273. Li, N. et al. Spatiotemporal constraints on optogenetic inactivation in cortical circuits. *eLife* **8**, e48622 (2019).
274. Yin, H. in *The Interdisciplinary Handbook of Perceptual Control Theory* (ed. Mansell, W.) 23–48 (Academic, 2020).
275. Wu, F. et al. Monolithically integrated μLEDs on silicon neural probes for high-resolution optogenetic studies in behaving animals. *Neuron* **88**, 1136–1148 (2015).
276. Valero, M., Zutshi, I., Yoon, E. & Buzsáki, G. Probing subthreshold dynamics of hippocampal neurons by pulsed optogenetics. *Science* **375**, 570–574 (2022).
277. Vöröslakos, M. et al. HectoSTAR μLED optoelectrodes for large-scale, high-precision in vivo opto-electrophysiology. *Adv. Sci.* **9**, 2105414 (2022).
278. Ko, E., Vöröslakos, M., Buzsáki, G. & Yoon, E. Dual-color μ-LEDs integrated neural interface for multi-control optogenetic electrophysiology. Preprint at *bioRxiv* https://doi.org/10.1101/2024.07.30.605927 (2024).
279. Roszko, D. A. et al. Foundry-fabricated dual-color nanophotonic neural probes for photostimulation and electrophysiological recording. *Neurophotonics* **12**, 025002 (2025).
280. Lakunina, A. et al. Neuropixels Opto: combining high-resolution electrophysiology and optogenetics. *Nature Methods* (in the press).
This work describes a high-density CMOS electrode array with on-shank photonic emitters, offering straightforward integration of large-scale electrophysiology and optogenetic stimulation.
281. Orban, G. et al. Single-die-level MEMS post-processing for prototyping CMOS-based neural probes combined with optical fibers for optogenetic neuromodulation. *Micromachines* **17**, 159 (2026).
282. Cohen, J. Y., Haesler, S., Vong, L., Lowell, B. B. & Uchida, N. Neuron-type-specific signals for reward and punishment in the ventral tegmental area. *Nature* **482**, 85–88 (2012).
283. Kravitz, A. V., Owen, S. F. & Kreitzer, A. C. Optogenetic identification of striatal projection neuron subtypes during in vivo recordings. *Brain Res.* **1511**, 21–32 (2013).
284. Economo, M. N. et al. Distinct descending motor cortex pathways and their roles in movement. *Nature* **563**, 79–84 (2018).
285. Lee, K., Carr, N., Perliss, A. & Chandrasekaran, C. WaveMAP for identifying putative cell types from in vivo electrophysiology. *STAR. Protoc.* **4**, 102320 (2023).
286. Schneider, A. et al. Transcriptomic cell type structures in vivo neuronal activity across multiple timescales. *Cell Rep.* **42**, 112318 (2023).
287. Valero, M. et al. Cooperative actions of interneuron families support the hippocampal spatial code. *Science* **389**, eadv5638 (2025).
288. Histed, M. H., Ni, A. M. & Maunsell, J. H. R. Insights into cortical mechanisms of behavior from microstimulation experiments. *Prog. Neurobiol.* **103**, 115–130 (2013).
289. Voigt, M. B., Hubka, P. & Kral, A. Intracortical microstimulation differentially activates cortical layers based on stimulation depth. *Brain Stimul.* **10**, 684–694 (2017).
290. Allison-Walker, T., Hagan, M. A., Price, N. S. C. & Wong, Y. T. Microstimulation-evoked neural responses in visual cortex are depth dependent. *Brain Stimul.* **14**, 741–750 (2021).
291. Ronchi, S. et al. Single-cell electrical stimulation using CMOS-based high-density microelectrode arrays. *Front. Neurosci.* **13**, 208 (2019).
292. Lima, S. Q., Hromádka, T., Znamenskiy, P. & Zador, A. M. PINP: a new method of tagging neuronal populations for identification during in vivo electrophysiological recording. *PLoS One* **4**, e6099 (2009).
293. Hikosaka, O. & Wurtz, R. H. Modification of saccadic eye movements by GABA-related substances. II. Effects of muscimol in monkey substantia nigra pars reticulata. *J. Neurophysiol.* **53**, 292–308 (1985).
294. Li, K. et al. Neuropeptides in the extracellular space of the mouse cortex measured by nanodialysis probe coupled with LC-MS. *Angew. Chem. Int. Ed. Engl.* **64**, e202509490 (2025).
295. Mu, X. et al. Implantable photonic neural probes with 3D-printed microfluidics and applications to uncaging. *Front. Neurosci.* **17**, 1213265 (2023).
296. Mu, X. et al. Nanophotonic neural probes for in vivo photostimulation, electrophysiology, and microfluidic delivery. *Microsyst. Nanoeng.* **12**, 100 (2026).
297. Perna, A., Angotzi, G. N., Berdondini, L. & Ribeiro, J. F. Advancing the interfacing performances of chronically implantable neural probes in the era of CMOS neuroelectronics. *Front. Neurosci.* **17**, 1275908 (2023).
298. Bashari, S., Jankowski, M. M. & Nelken, I. The representation of regularity and randomness in auditory cortex of awake rats. Preprint at *bioRxiv* https://doi.org/10.1101/2025.04.09.647967 (2025).
299. Erofeev, A., Antifeev, I., Vinokurov, E., Bezprozvanny, I. & Vlasova, O. An open-source wireless electrophysiology system for in vivo neuronal activity recording in the rodent brain: 2.0. *Sensors* **23**, 9735 (2023).
300. Kwon, Y. W. et al. Power-integrated, wireless neural recording systems on the cranium using a direct printing method for deep-brain analysis. *Sci. Adv.* **10**, eadn3784 (2024).
301. Lee, B. et al. An inductively-powered wireless neural recording and stimulation system for freely-behaving animals. *IEEE Trans. Biomed. Circuits Syst.* **13**, 413–424 (2019).
302. Zhao, S. et al. Tracking neural activity from the same cells during the entire adult life of mice. *Nat. Neurosci.* **26**, 696–710 (2023).
303. Yuan, A. X. et al. Multi-day neuron tracking in high-density electrophysiology recordings using earth mover's distance. *eLife* **12**, RP92495 (2024).
304. van Beest, E. H. et al. Tracking neurons across days with high-density probes. *Nat. Methods* **22**, 778–787 (2025).
305. Brunner, C. et al. A platform for brain-wide volumetric functional ultrasound imaging and analysis of circuit dynamics in awake mice. *Neuron* **108**, 861–875 (2020).
306. Hay, E., Hill, S., Schürmann, F., Markram, H. & Segev, I. Models of neocortical layer 5b pyramidal cells capturing a wide range of dendritic and perisomatic active properties. *PLoS Comput. Biol.* **7**, e1002107 (2011).
307. Wang, Q. et al. The Allen Mouse Brain Common Coordinate Framework: a 3D reference atlas. *Cell* **181**, 936–953.e20 (2020).
308. Claudi, F. et al. Visualizing anatomically registered data with brainrender. *eLife* **10**, e65751 (2021).
309. Ottenheimer, D. J., Hjort, M. M., Bowen, A. J., Steinmetz, N. A. & Stuber, G. D. A stable, distributed code for cue value in mouse cortex during reward learning. *eLife* **12**, RP84604 (2023).
310. Kauvar, I. et al. Conserved brain-wide emergence of emotional response from sensory experience in humans and mice. *Science* **388**, eadt3971 (2025).
311. Bennett, C. et al. Map of spiking activity underlying change detection in the mouse visual system. Preprint at *bioRxiv* https://doi.org/10.1101/2025.10.17.683190 (2025).
312. Siegle, J. H. et al. Open Ephys: an open-source, plugin-based platform for multichannel electrophysiology. *J. Neural Eng.* **14**, 045003 (2017).
313. Lopes, G. et al. Bonsai: an event-based framework for processing and controlling data streams. *Front. Neuroinformatics* **9**, 7 (2015).
314. Chung, J. E. et al. A fully automated approach to spike sorting. *Neuron* **95**, 1381–1394 (2017).
315. Jain, A. et al. UnitRefine: a community toolbox for automated spike sorting curation. Preprint at *bioRxiv* https://doi.org/10.1101/2025.03.30.645770 (2025).
316. Fuglstad, J. G., Saldanha, P., Paglia, J. & Whitlock, J. R. Histological e-data registration in rodent brain spaces. *eLife* **12**, e83496 (2023).
317. Peters, A. J. petersaj/AP_histology: AP_histology v2.0.0. *Zenodo* https://doi.org/10.5281/zenodo.18746423 (2026).
318. Denker, M., Yegenoglu, A. & Grün, S. Collaborative HPC-enabled workflows on the HBP collaboratory using the Elephant framework. In *Neuroinformatics 2018* https://doi.org/10.12751/incf.ni2018.0019 (2018).
319. Viejo, G. et al. Pynapple, a toolbox for data analysis in neuroscience. *eLife* **12**, RP85786 (2023).

Acknowledgements
The authors thank A. Li, C. Schoonover and C. Mora Lopez for helpful suggestions and feedback on this manuscript. They thank A. Li for help in preparing the publicly available data replotted in Fig. 5. This work was supported by The Pew Biomedical Scholars Program (N.A.S.), a Klingenstein–Simons Fellowship in Neuroscience (N.A.S.) and the National Institutes of Health (NIH) (U01NS113252 to N.A.S.). Additional funding was provided by the Allen Institute.

Author contributions
The authors contributed equally to all aspects of the article.

Competing interests
The authors declare no competing interests.

Additional information
Peer review information *Nature Reviews Neuroscience* thanks Emily Aery Jones, Edward Chang, Matthias Hennig and the other, anonymous, reviewer(s) for their contribution to the peer review of this work.

Publisher's note Springer Nature remains neutral with regard to jurisdictional claims in published maps and institutional affiliations.

Related links
Blackrock Neurotech: https://blackrockneurotech.com/
NeuroNexus: https://www.neuronexus.com/
Neuropixels: https://www.neuropixels.org/
Plexon: https://plexon.com/